

Host-Guest Interaction of calix[4]arene derivatives with
Metformin

Report submitted to the Central University of Punjab

For the award of

Master of Sciences

In

CHEMISTRY

BY

Harshita Gupta

Supervisor

Dr. J. Nagendra Babu



Department of Chemical Sciences

School of Basic and Applied Sciences

Central University of Punjab, Bathinda

May, 2018

CERTIFICATE

I declare that the report entitled “HOST-GUEST INTERACTION OF CALIX[4]ARENE DERIVATIVES WITH METFORMIN” has been prepared by me under the guidance of Dr. J. Nagendra Babu, Assistant Professor, Department of Chemical sciences, School of Basic and Applied Sciences, Central University of Punjab. No part of this report has formed the basis for the award of any degree or fellowship previously.

Harshita Gupta

Department of Chemical Sciences

School of Basic and Applied Sciences

Central university of Punjab, Bathinda – 151001

Date:

CERTIFICATE

I certify that HARSHITA GUPTA has prepared her report entitled “HOST-GUEST INTERACTION OF CALIX[4]ARENE DERIVATIVES WITH METFORMIN” for the award of M.Sc. degree in subject Chemistry under the faculty of Chemical Sciences of Central University of Punjab, under my supervision and guidance. She has carried out this work at the Department of chemical sciences, School of Basic and Applied Sciences, Central University of Punjab.

Dr. J. Nagendra Babu

Assistant Professor

Department of Chemical Sciences

School of Basic and Applied Sciences

Central University of Punjab, Bathinda – 151001

Date:

ABSTRACT

Host-Guest Interaction of Calix[4]arene Derivatives with Metformin

Name of student : Harshita Gupta
Registration number : 16mscchm13
Degree for which submitted : M.Sc. in Chemistry
Name of supervisor : Dr. J. Nagendra Babu
Name of Department : Chemical Sciences
Name of school : Basic and Applied Sciences
Keywords : Calix[4]arene, Host-guest complex, Metformin, Benesi-Hildebrand equation.

ABSTRACT

Calix[4]arene was lower rim functionalized to furnish receptor 2-3 and 4-6, containing propyl and cyanomethoxy moieties, respectively. The receptors were characterized by FTIR, ^1H and EI-MS. UV-visible studies were performed with receptor 2-6 cone ($1 \times 10^{-4}\text{M}$) upon addition of metformin (1×10^{-5} - $1 \times 10^{-3}\text{M}$). Upon addition of metformin the UV-Visible absorption showed a hyperchromic shift. The 1:1 Host-Guest complexation studied by Benesi-Hildebrand equation showed a stability constant in the range 2×10^4 - $10 \times 10^4 \text{M}^{-1}$.

(Harshita Gupta)

(Dr. J. Nagendra Babu)

ACKNOWLEDGEMENT

This report is the end of my journey in obtaining my Post Graduate. I have not traveled in a vacuum in this journey. This report has been kept on track and been seen through to completion with the support and encouragement of numerous people including my well-wishers, my friends, colleagues and various institutions. At the end of my report I would like to thank all those people who made this report possible and an unforgettable experience for me. At the end of my report, it is a pleasant task to express my thanks to all those who contributed in many ways to the success of this study and made it an unforgettable experience for me.

I consider myself blessed to work under the supervision of, “**Dr. J. Nagendra Babu**”,

who has supported me throughout my report with his patience and knowledge whilst allowing me the room to work in my own way. I attribute the level of my Master’s degree to his encouragement and effort and without him this report, too, would not have been completed or written. One simply could not wish for a better or friendlier supervisor. Under his guidance I successfully overcame many difficulties and learned a lot. Let me place on record my gratitude to all my former teachers who made me what I am today “**Dr. Rakesh Kumar**”, “**Dr. Rajesh Kumar**” and “**Dr. Krishna Kanta Haldar**”, “**Dr. Rajendra Singh Dhayal**”, “**Dr. Biplab Banerjee.**” for the useful comments, remarks and engagement through the learning process of this master’s course.

It’s my pleasure to acknowledge **Indu Prakash Pandey** for their constant moral support. He was always beside me during the happy and hard moments to push me and motivate me. I will be grateful forever for his love.

I wish to thanks seniors **Mansi Garg, Samreet, Pavneet kaur, Archana Kumari Sharma, Rabindra Kumar** for their great help during the whole study.

I would also like to extend huge, warm thanks to my roommate, **Rabiya**. I am indebted to some of my good friends, **Mange Ram Soni, Bhupender Kumar Mehta** for their valuable help and support.

I express my deepest appreciation to my class mates, for the joyful gatherings and all their supports.

I would like to acknowledge my other friends **Niharika**, **Dr. Meha** for their moral support and motivation, which drives me to give my best.

I wish to acknowledge to all my juniors for their valuable help during the whole study.

Last but not least, I would like to pay high regards to my **papa** and **mummy**, my brother **Rishi Kant** and my sister **Monica** for their sincere encouragement and inspiration throughout my research work and lifting me uphill this phase of life. I owe everything to them. Words are but a few to express the deep appreciation to my father "**R.C Gupta**" and my lovely mother "**Beena Gupta**" and all other members of my family and all my well-wishers for their indispensable encouragement and their interest in my work, for many sacrifices they have made for me. I thank God Almighty for blessing me with such caring parents.

(Harshita Gupta)

*Dedicated
To my
Parents*

TABLE OF CONTENTS

Sr. No.	Content	Page No.
1	Introduction (Chapter I)	01-03
2	Review of Literature (Chapter II)	04-17
3	Materials and Methods (Chapter III)	18-22
4	Results and Discussions (Chapter IV)	23-38
5	Conclusions (Chapter V)	39-40
6	References	41-43

LIST OF TABLES

Table No.	Description of Table	Page No.
1	Stability constant for host-guest complexation of calix[4]arene derivative H-2-6 with metformin.	38

LIST OF SCHEME

Table No.	Description of Scheme	Page No.
4.1	Synthesis of calix[4]arene derivative in cone and 1,3-alternate conformation	32

LIST OF FIGURES

Figure No.	Description of figure	Page No.
1	Depicting the structure and shape of calixarene	5
2	Conformations of calix[4]arene (a) cone (b) Partial cone (c)1,3-alternate and (d) 1,2-alternate	7
3	Schematic representation of a vesicle – to- micelle transition of 2b with a pH and subsequent release of encapsulated calcein	8
4	Side on binding of 4 within π -basic cavity of 3	10
5	Representation of the structure of 5, Ce6 guest molecule, and formation of the supramolecular polymeric micelles based on host-guest interaction	11
6	The acid dissociation equilibrium for metformin	12
7	The host-guest complexation of metformin and cucurbit[7]uril to form a 2:1 (H:G) complex as revealed by NMR and ESI-MS	14
8	The host-guest complexation of metformin and p-sulfonatocalix[4]arene	17
9	FTIR of calix[4]arene derivative H-2	25
10	¹ H NMR spectra of H-2	25
11	FTIR of calix[4]arene derivative H-3	26
12	¹ H NMR spectra of H-3	27
13	FTIR spectra of calix[4]arene derivative H-4	28
14	¹ H NMR spectra of H-4	28
15	FTIR spectra of calix[4]arene derivative H-5	29

16	¹ H NMR spectra of H-5	30
17	FTIR spectra of calix[4]arene derivative H-6	31
18	¹ H NMR spectra of H-6	31
19	UV-Visible absorption changes upon addition of 0 to 10 equivalent metformin to H-2 (1×10^{-4}) in methanol: chloroform 9:1 (v/v)	33
20	Benesi-Hildebrand plot of H-2 for metformin determined by UV-Vis method	33
21	UV-Visible absorption changes upon addition of 0 to 10 equivalent metformin to H-3 (1×10^{-4}) in methanol: chloroform 9:1 (v/v)	34
22	Benesi-Hildebrand plot of H-3 for metformin determined by UV-Vis method	35
23	UV-Visible absorption changes upon addition of 0 to 10 equivalent metformin to H-4 (1×10^{-4}) in methanol: chloroform 9:1 (v/v)	36
24	Benesi-Hildebrand plot of H-4 for metformin determined by UV-Vis method	36
25	UV-Visible absorption changes upon addition of 0 to 10 equivalent metformin to H-6 (1×10^{-4}) in methanol: chloroform 9:1 (v/v)	37
26	Benesi-Hildebrand plot of H-6 for metformin determined by UV-Vis method	37

LIST OF ABBREVIATIONS

Sr. No	Full Form	Abbreviation
1.	Dimethylformamide	DMF
2.	Deuterated Chloroform	CDCl ₃
3.	Fourier Transform-Infrared spectrophotometer	FTIR
4.	Nuclear Magnetic Resonance	NMR
5.	Electrospray ionization	ESI
6.	Distilled water	D.W
7.	Photosensitizer	PS
8.	Chlorin e6	Ce6
9.	5,11,17,23,-De-tert-butyl-25,26,27,28-tetra-poly(ethylene glycol)calix[4]arene	DC4-PEG
10.	Ion-Selective Electrodes	ISE
11.	Isothermal Titration Calorimetry	ITC
12.	Deuterium oxide	D ₂ O
13.	Sulphonated[n]calixarenes	SCnAs
14.	Thin layer chromatography	TLC
15.	Sodium Hydride	NaH
16.	Ultra-violet	UV
17.	Propyl Iodide	PrI

CHAPTER I

INTRODUCTION

Introduction

Supramolecular chemistry is the study of non-covalent interactions between molecules to assemble, function and recognize each other. This assembly of molecules is driven by intermolecular forces responsible for interaction such as hydrogen bonding, metal coordination, hydrophobic forces, van der waal interaction, π - π interaction and electrostatic interaction (Steed and Atwood 2013). These intermolecular interactions in supramolecular recognition, with hosts designed on the principles of pre-organization and complementarity with respect to the guest, opens up wide range of applications. These applications include optical sensor devices, drug delivery systems, non-linear optical materials, liquid crystals, magnetic material and electronic devices. Supramolecular system functionalized to achieve efficient drug delivery system that alters physiochemical and pharmacokinetic characteristics of drugs are immensely studied (Yang 2011). Drug delivery system with features of sustained, controlled and targeted release are highly desirable (Zhou et al. 2015). The design of molecular hosts for carrying different drug molecules is a challenge, as these drugs comprise of polar organic functional moieties as well as hydrophobic groups to maintain the K_{ow} (octanol/water partition coefficient) of the drug, which is essential for the transport of drug as well as its action. Thus, suitable container molecules with hydrophobic cavities with tailor made scaffold functionalized for complementarity based drug recognition is the need of the hour.

Different macrocyclic systems have been employed in the design of host-guest based drug delivery systems that include cyclodextrin, calixarene, cucurbituril, and pillarene. (Duan et al. 2013) (MacGillivray and Macartney 2013) (Wang et al. 2012). Cyclodextrin has been extensively studied in drug encapsulation and binding, however its functionalization is not that easy (Roselet and Premakumari 2015). On the other hand, calixarenes are a class of 1_n -metacycophanes which is a versatile guest for the design of drug recognition system. Calixarene scaffold is a bowl or cone shaped supramolecular macrocycle consisting of phenol units linked at ortho position by methylene bridge. Calix[n]arenes ($n= 4-20$) are economical to synthesize by a simple condensation of para-substituted phenol and formaldehyde. Calix[4]arene, the smallest of all the calixarene is easily functionalized on the lower rim, upper rim and methylene bridges apart from being

capable of adopting various conformation and forming inclusion complexes using its basic π -tube cavity (Wheate et al. 2009). The conformation of calix[4]arene could be tailored to design host for desired guest molecule binding. Calix[4]arene provides a microenvironment, in which, appropriate size of non-polar moieties would enter to form inclusion complex. The inclusion into the cavity leads to change in physiochemical properties of guest molecules that are beneficial in drug delivery (Wheate et al. 2009). Calixarene have been widely studied for drug delivery systems in the form of carrier. It has been observed that calix[4]arene-drug recognition has been studied only with calix[4]arenes in cone conformation. However there are few reports on the study of the influence of conformation of calix[4]arene on drug recognition. Thus, herein we have studied the influence of conformation and lower rim functionalization of calix[4]arene on the binding of the antidiabetic drug, metformin by UV-Visible studies.

CHAPTER II
REVIEW OF LITERATURE

Review of Literature

2.1 Calixarene:

'Calixarene' is well known class of macrocyclic compound, the term was presented by C.D Gutsche for the cyclic oligomers which are formed from the condensation of formaldehyde with p-alkylphenols in alkaline conditions (Gutsche et al. 1982). Calixarene are cyclic oligomers of derivatized benzenes linked by methylene units (**Figure 1**). The basic structural features of these architecturally important cup-shaped macrocycles consisting of upper rim, annulus and lower rim, are clearly key elements for future design purposes. Since their discovery they have structural attributes, both geometric and electronic, that is conducive to host-guest complexation. Their ease of synthesis allows various synthetic modifications of both upper and lower rim (Gutsche and David 2008).

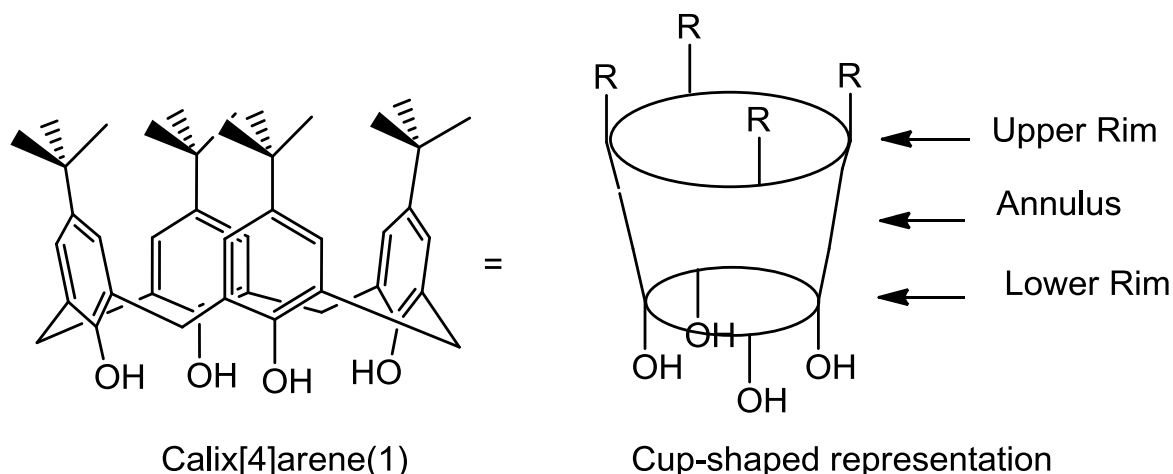


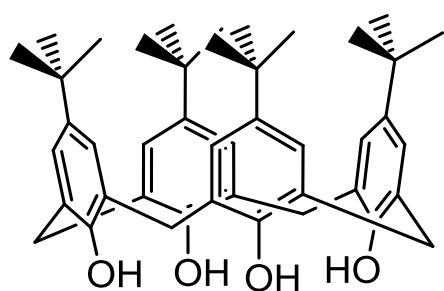
Figure 1: Depicting the structure and shape of calix[4]arene.

Calixarene molecule have cup like shape and can accommodate smaller guest molecules within itself, binding by the phenomenon called inclusion. Calixarene molecules belong to the class of cavitands because it has hydrophobic cavities that can hold smaller molecules and ions (Gutsche and David 2008). The inclusion in the calixarene container could be tailor-made either by increasing the number of repeating monomer units i.e. methylene phenol unit or changing the conformation of the calixarene. By conformation, it is meant that the phenolic units of calixarene can rotate on the axis of the two bridging methylenes leading to a syn- and anti-orientation of the phenolic functional moiety w.r.t each other, the rotation is called

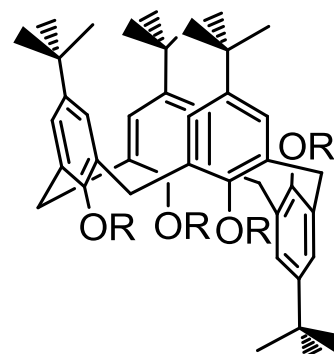
through annulus rotation and the orientation adopted by each phenolic moiety would render a different conformation to the individual molecule of calixarene which represents the conformations of calixarene. For example, in case of calix[4]arene, the syn and anti orientation of the phenolic moieties of calix[4]arene leads to four conformation commonly known as cone, partial-cone, 1,3-alternate and 1,2-alternate conformation (**Figure 2**). **1** possess four stereo-centres at the bridging points of the macro cycle. Different isomeric arrangements at these points produce a different conformation in the macrocycle (**Figure 2**).

When the phenolic hydroxyl groups on the lower rim of the t-butylcalix[4]arenes are functionalized this locks the macrocycle in a single conformation (Liu et al. 2003). The conformation interconversion is sterically hindered because the pendant chains blocked the passage through the annulus. Calixarenes containing free intraannular OH groups are conformationally mobile in solution at room temperature. This effect is considerably more pronounced in polar solvents, such as acetone, acetonitrile and pyridine, than in non-polar solvents, such as chloroform and benzene. It may be explained in terms of the inversion barrier in which polar- solvents are able to disrupt the intramolecular hydrogen bonds that contribute in maintaining the calixarene in the cone conformation.

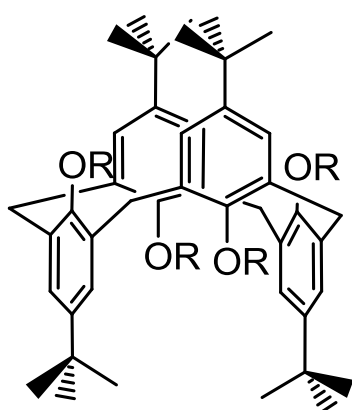
In calix[4]arene (**1**) in which one or more of the hydrogens of the OH groups are replaced by other groups frequently exist in the cone conformation, same observed for the monomethyl ether of tert-butylcalix[4]arene. The conformational inversion barrier is almost identical to that of unsubstituted tert-butylcalix[4]arene (Stewart et al. 1995).



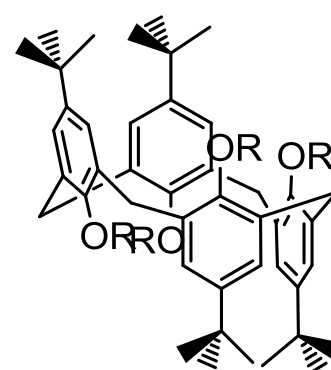
A-Cone



B-Partial Cone



C-1,3-alternate



D-1,2-alternate

Figure 2: Conformations of calix[4]arene (A) Cone (B) Partial Cone (C) 1,3-alternate and (D) 1,2-alternate.

Lee et al., (2004) synthesized amphiphilic tetramer that is calixarene (**2a-c**) functionalized on the upper rim with a dibranched hydrophilic chain via amine group and lower rim connected to four lipophilic decyl chains which can establish aggregates with increased stability and pH responsive character (Lee et al. 2004). The changes in the size and structure of the aggregates from large vesicles to small spherical micelles could be brought about by small variation in physicochemical environment like pH or hydrophilic chain length (**Figure 3**). The effect on the pH during structure change from the vesicular structure to micellar structure was investigated by DLS measurement. Measurements show that drop in pH will decrease the size of aggregate from 36 nm at pH 7 to 6 nm at pH 5, this transition behaviour helps in the release of guest molecules in response to a decrease in pH (Lee et al. 2004). This stimuli response was demonstrated by using fluorescent dye calcein as guest encapsulated in the host, which is released

in response to decrease in pH accompanied by an increase in fluorescence emission. Hence it can be used for selective drug delivery in tissues of a lower pH value.

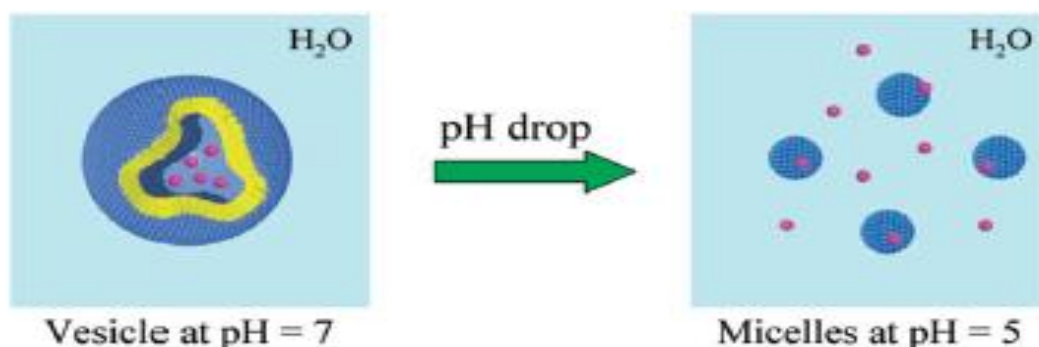
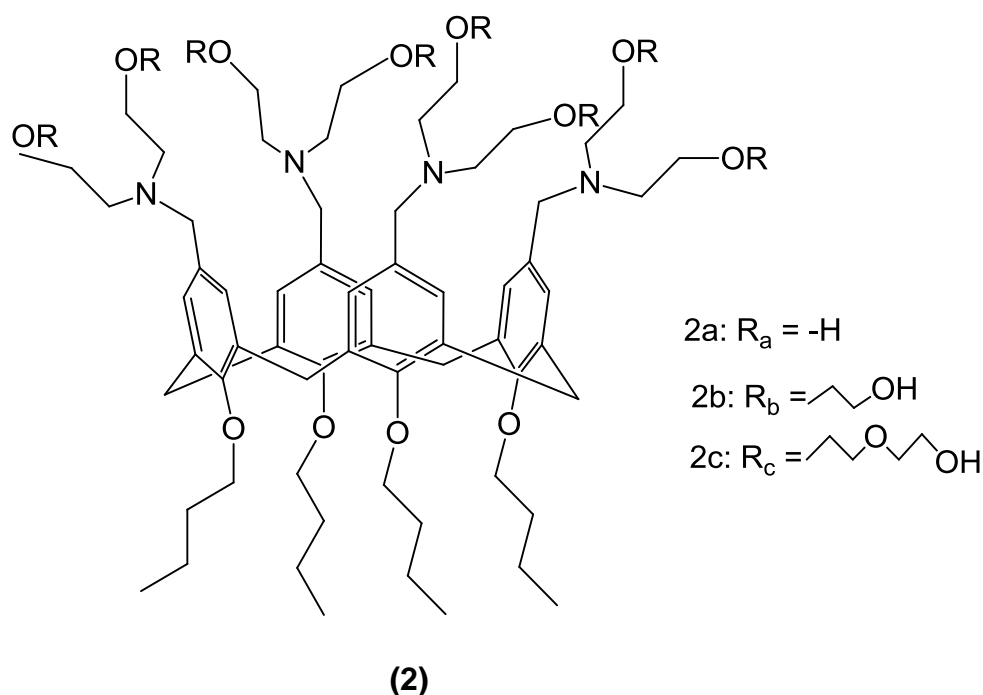
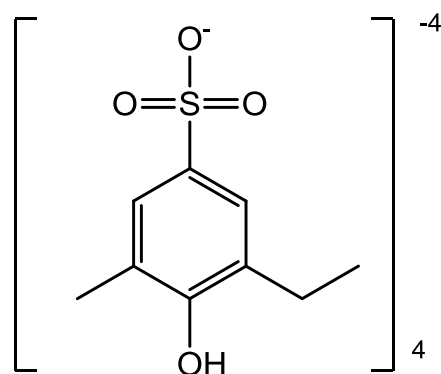


Figure 3: Schematic representation of a vesicle-to-micelle transition of **2b** with a pH and subsequent release of encapsulated calcein (Lee et al. 2004).

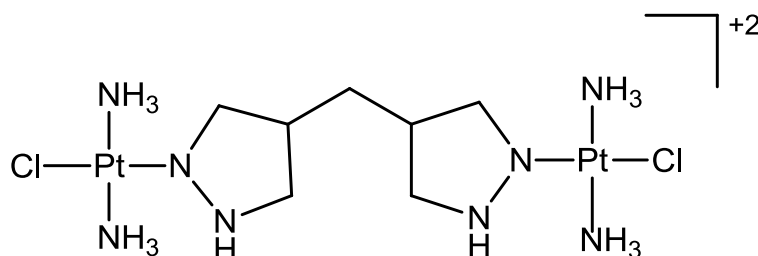


Wheate and coworkers constructed a drug delivery vehicle based on host-guest complexation of *p*-sulphonatocalix[4]arene (**3**) to the dinuclear platinum complex (**4**) via side-on binding (Wheate et al. 2009). ESI-MS study confirms the 1:1 binding stoichiometry. NMR study showed a large chemical shift of di-Pt complex, when di-Pt complex **4** was titrated with **3**. The protons H-3, H-5, and CH₂ of **4**

showed a shift of ($\Delta\delta$) 0.4, 1.05, 1.15ppm upfield at 0.5:1 ratio (**3**:**4**). On further addition of **3** to the solution of **4** upto the ratio of 1:1, the metal- complex resonance shows a downfield chemical shift with two separate shift for NH_3 protons of **4**. The downfield shift of di-Pt is due to the shielding provided within the cavity of **3**. Both amine protons have different downfield shift because amine group in **4** is bonded to sulphate group of **3** hydrogen bonding, due to which its rotation is restricted whereas other is not. Interaction of **4** with **3** was confirmed by Rotating Frame Over Hauser Effect (ROE), the NMR study established a side-on binding between **3** and **4** because of the insufficient opening at lower rim, as shown in molecule **3**. The proposed binding that is stabilized by ion-ion interaction between sulphate group and the platinum ion or ion-dipole interaction between amine and sulphate groups. As one set of the moieties of dinuclear Pt complex interacts, the binding constant is low. This is generally required for drug delivery. (**3**) and (**4**) form inclusion complex which will dissociate easily and the system will release di-Pt into the body due to high content of blood serum.



(3)



(4)

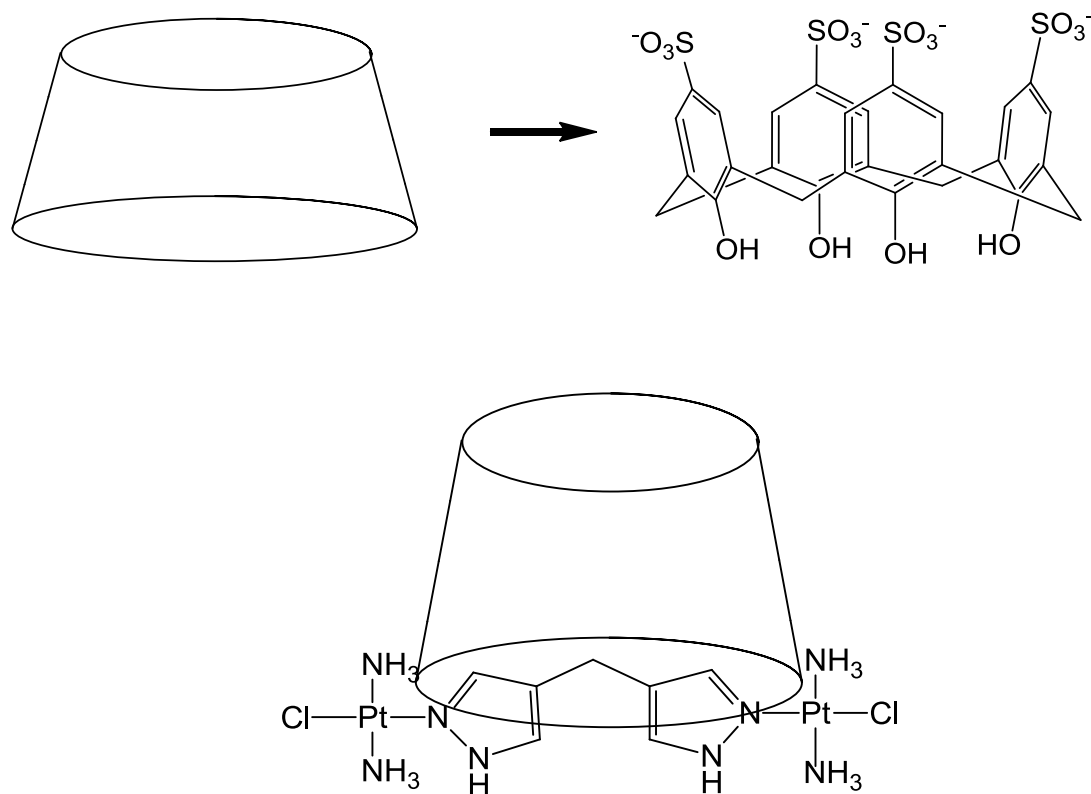


Figure 4: Side on binding of 4 within the π -basic cavity of 3.

Tu et al., (2011) studied drug delivery system by designing a novel self-assembly of a supramolecular amphiphilic polymer based on lower rim PEGylated calix[4]arene (Tu et al. 2011). Calix[4]arene derivatives can encapsulate hydrophobic photosensitizers (PSs), via host guest complexation and self-assembly into supramolecular amphiphiles based polymeric micelles in aqueous solution (**Figure 5**), which avoids the aggregation of PSs. **Ce6** is a natural photosensitizer derived from chlorophyll. This host-guest complexation was monitored by ^1H NMR titrations at different host/ guest mole ratios. The complexation between PEGylatedcalix[4]arene (**5**) and Chlorin e6 (**Ce6**) was monitored by ^1H NMR at different host/ guest ratio. Signals of the **Ce6** protons H_α , H_β , C_1 , C_3 , C_5 , C_4 , C_2 showed a downfield shift with increase in concentration of host/guest ratio. For signals belonging to H_7 , H_8 , C_8 , C_7 and C_8 showed an upfield shift whereas meso- H_5 remained unchanged because of the shielding provided by the cavity of **5**, when **Ce6** binds to **5**. Hence it indicates 1:1 inclusion complex of **Ce6** and **5**. According to Job's plot result, there is a formation of 1:1 inclusion complex of **Ce6** guest with **5** host. This supramolecular polymeric micelles is

utilized as a safe drug carrier with low cytotoxicity and can be delivered into tumour cell. The inclusion complex **5-Ce6** exhibit more efficient photodynamic therapy than free **Ce6**. Flow cytometry findings show that when cell is exposed to free Ce6 showed less fluorescence in comparison to the cells exposed to **5-Ce6** micelles in the cytoplasm. Thus, **5** could be used in photodynamic therapy for efficient drug delivery to inhibit growth of HeLa cells.

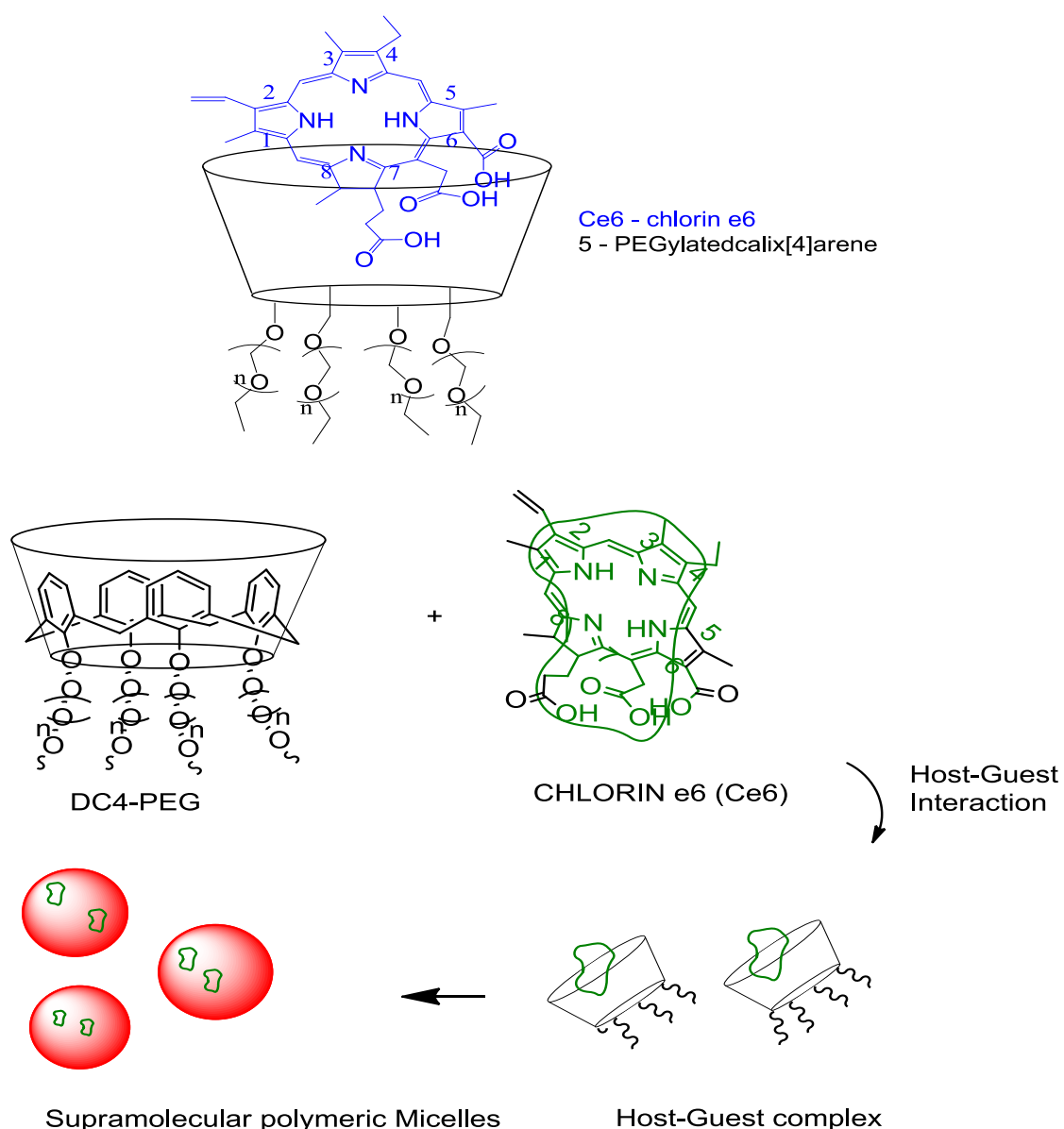


Figure 5: Representation of the structure of **5**, Ce6 guest molecule, and formation of the supramolecular polymeric micelles based on host-guest interaction (adopted from (Tu et al. 2011)).

Metformin and its interaction with various container molecules:

Metformin is the first line therapy of type-2 Diabetes. It belongs to the class of biguanidinium (Roselet and Premakumari 2015). Metformin is an oral antihyperglycaemic agent, widely used in the treatment of type-2 diabetes. Metformin belongs to the class of biguanidiums developed from galegina found in *Galega officinalis*, a herbal medicine in Europe, rich in guanidine (Scheen 1996). Guanidine derivative were used to treat diabetes in the 1920s and 1930s and its use was discontinued due to its toxicity, but it was rediscovered in 1940s and proved useful to lower blood glucose level. Metformin has its dissociation constant value of 2.8 (pK_{a1}) and 11.5 (pK_{a2}) as shown in (Figure 6) (Guo et al. 2012). Therefore, it exist as cationic species at physiological pH. It is white to off-white in color, crystalline compound with a molecular formula of $C_4H_{11}N_5$ and molecular weight is 129.163 g/mol (Tripathi 2013). Metformin is soluble in water but it is insoluble in ether, acetone and chloroform. Metformin is not used for passive diffusion via cell membrane because it is hydrophilic in physiological conditions.

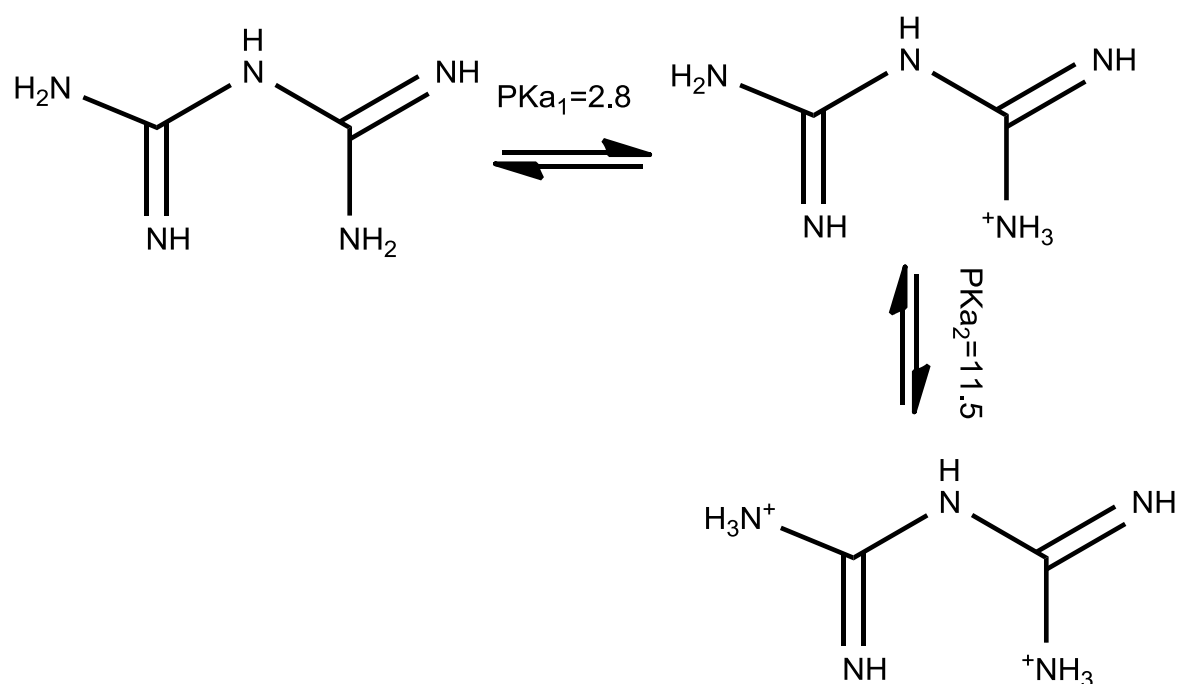


Figure 6: The acid dissociation equilibrium for metformin.

Clinical pharmacology

There are three types of diabetes; Type-1 Diabetes, it is caused when β -cell in the islet of Langerhans tissue of pancreas do not produce insulin in the body due to auto immune destruction of β -cells (Chang-Chen et al. 2008); Gestational Diabetes, it is caused during pregnancy, anti-insulin hormones are produced due to which high glucose levels are observed in the blood; type-2 Diabetes, it is caused when there is reduction in the insulin action as the body tissues fail to respond to insulin being produced in the body i.e. insulin resistance.

Metformin is the first line therapy of type-2 Diabetes, its pharmacologic mechanism of action are different from other classes of oral antihyperglycemic agent, its medication improves the glucose tolerance with type2 diabetic patient, by lowering basal and postprandial plasma glucose.

Metformin works through three methods; decrease in blood glucose by decrease in hepatic glucose production, decrease in intestinal absorption of glucose and by improving insulin sensitivity by increasing uptake of peripheral glucose and its utilization. Glucose is responsible for growth and development of tissues as well as proper functioning of the body. All of the three actions of metformin is activated by the ability of metformin to activate AMP-activated protein kinase or AMPK. AMPK is a liver enzyme that has a crucial role in insulin signaling, whole body energy balance and the metabolism of glucose and fats. Metformin also increases AMPK activity in skeleton muscles as a result of activating AMPK, it facilitates the opening of GLUT 4 in the plasma membrane which results in the insulin independent glucose uptake. Insulin lowers blood glucose levels without causing hypoglycemia. GLUT 4 is the insulin sensitive glucose transporter that occurs only in the muscle and adipose tissue.

MacGillivray and Macartney., (2013) studied host-guest complexation of cucurbit[7]uril with Biguanidinium cations namely, metformin, phenformin, alexidine, chloroformin in aqueous solution.(MacGillivray and Macartney 2013). The complexation of metformin (**6**) by cucurbit[7]uril (**7**) were followed by using ^1H NMR and ESI-MS techniques. ESI mass spectroscopy determined stoichiometric of the host-guest complex of **6** with **7** in D_2O was observed to show both stoichiometries 1:1 and 2:1 (H:G). ^1H NMR study unraveled the stoichiometric and

stability constant of the **7** host guest complex and identify the site of the guest over which **7** is positioned. The ^1H NMR showed a downfield chemical shift for guest protons outside of the cavity and upfield shift for encapsulated guest protons because of the shielded environment provided by the cavity of the host **7**. The linear chemical shift is observed until a **7/6** ratio of 0.50 is reached, leading to the formation of 2:1 host-guest complexation but at higher concentration of guest it transforms to 1:1 host-guest complex. The observed chemical shift for 2:1 host guest complex. (**Figure 7**) that is $\sim 0.17\text{ppm}$, suggest that two **6** guest are partially encapsulated, with one fully encapsulated whereas other bounded to the portal externally via hydrogen bonding and ion-dipole interactions.

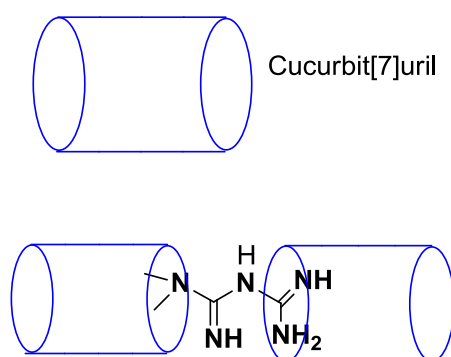
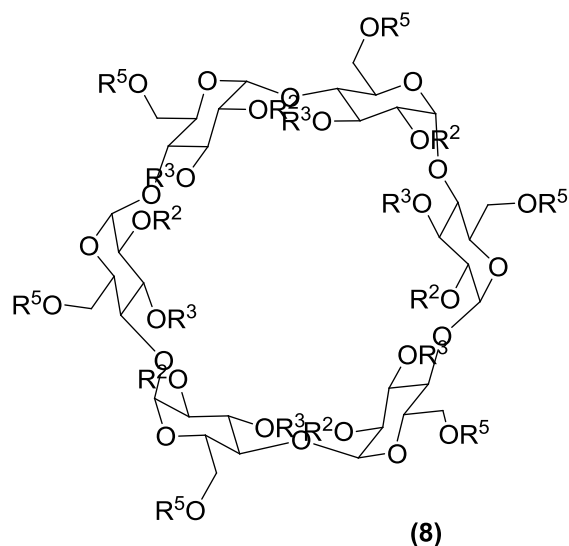


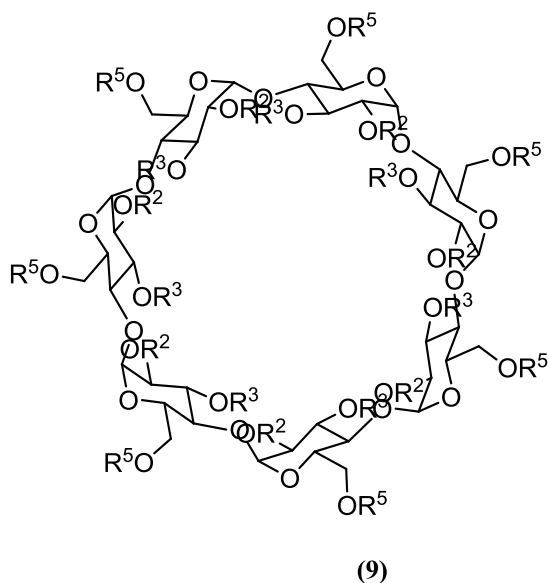
Figure 7: The host-guest complexation of metformin and Cucurbit[7]uril to form a 2:1 (H:G) complex as revealed by NMR and ESI-MS.

Kataky et al.,(1994) conducted a study on the alkylated cyclodextrins(**8a-c**) and (**9a-b**) complexation with guanidinium ions and its protonated derivatives, metformin and phenformin potentiometrically (Kataky et al. 1994). Response of cyclodextrin (**8**) to the guanidinium ion in presence and absence of interference ions was done on standard electrode with 1mM NH_4Cl internal filling solution. Selectivity of different **8a-c** towards guanidinium ions over other ions was measured by the fixed interferant method. Result of the response of electrode to the guanidinium ion showed that all cyclodextrins **8a-c** showed Nernstian response and a good ISE for detection hence the binding is not specific, the ion is able to interact with all type of alpha and α -**8a-c** and β -**9a-b** ring via multi N-H---O< interactions with the 2,6-oxygen lone pair because ion is too small to interact peripherally with **8a-c** as there is no significant difference in response has been observed during interaction between the **8** with or without OH groups. **8a-c** prefer to show more affinity to large cations with diffuse charge and less affinity to small

cation with more charge. Therefore, it has clinical applications to show selectivity towards the guanidinium over sodium ion of highest concentration in blood. ESI MS further show that there is formation of a 1:1 inclusion complex between 2,6,-didodecyl- β -cyclodextrin and guanidinium ion via single peak, no other binding with ammonium ion was observed even in the excess concentration of **8**.



- 8a :R² = R⁵ = Octyl, R³= OH
 8b :R² = R⁵ = Octyl, R³= octyl/OH
 8c :R² = R⁵ = Octyl, R³= octyl/methyl



- 9a :R²=R³=R⁵= Octyl
 9b :R²=R⁵= Dodecyl, R³=OH

Guo et al., (2012) conducted a study on selective binding of p-sulfonatocalix[4/5]arene with biguanidinium guests; metformin and phenformin (Guo, 2012). Investigation involved binding geometries, abilities and thermodynamic parameters for the host-guest complexation and it was done by ^1H and ^2D NMR spectroscopy, X-Ray crystallography, and isothermal titration calorimetry (ITC) studies. ^1H NMR spectroscopic experiment in D_2O clearly showed inclusion complex between SCnAs and guanidinium cation. The ^1H NMR study of metformin binding to sulphonatocalix[4/5]arene showed a upfield shift in case of protons of methyl group in **6**. This upfield shift was accounted to the ring current effect of the aromatic nuclei of **3**. Electrostatic and hydrogen binding are the expected interactions taking place between the negatively charged sulfonate and methyl group of **6** and aromatic portion of the **6** is captured in the hydrophobic cavity of the **3** and the biguanidinium portion is captured by the upper rim sulfonate groups. Single-crystal X-ray studies revealed structure of Complex of **3** with **6** to crystallize in monoclinic space group $\text{P}2_1/\text{n}$, where two crystallographically distinct **3**, four metformin, and 18.25 water molecules are arranged in the assymmetric unit. In host-guest inclusion structure, the methyl group of metformin guest is captured into the cavity of **3** through C-H- π interaction whereas the guanidinium group captured by the sulfonates group on the **3** through hydrogen bonding (**Figure 8**). ITC measurements was also done which conclude that complexation of host with guest is influenced by the surroundings ions. Two factors contribute to the higher stability of the complex for diprotonated biguanidinium ion i.e., enthalpy and entropy. ITC measurements under acidic and neutral conditions showed strong binding affinity of **3** for **6** at pH 2 than at pH 7.2 due to the protoned state of guanidinium guest. The binding involving protonated state of metformin is accounted to the dissolution effect, which is reflected from the entropy change ($T\Delta\text{S}=4.16\text{KJmol}^{-1}$). However, in deprotonated state, **6** showed more charge interactions and hydrogen bonding with sulfonate groups of **3**, shown by the enthalpy change ($\Delta\text{H}=-3.17\text{KJmol}^{-1}$).

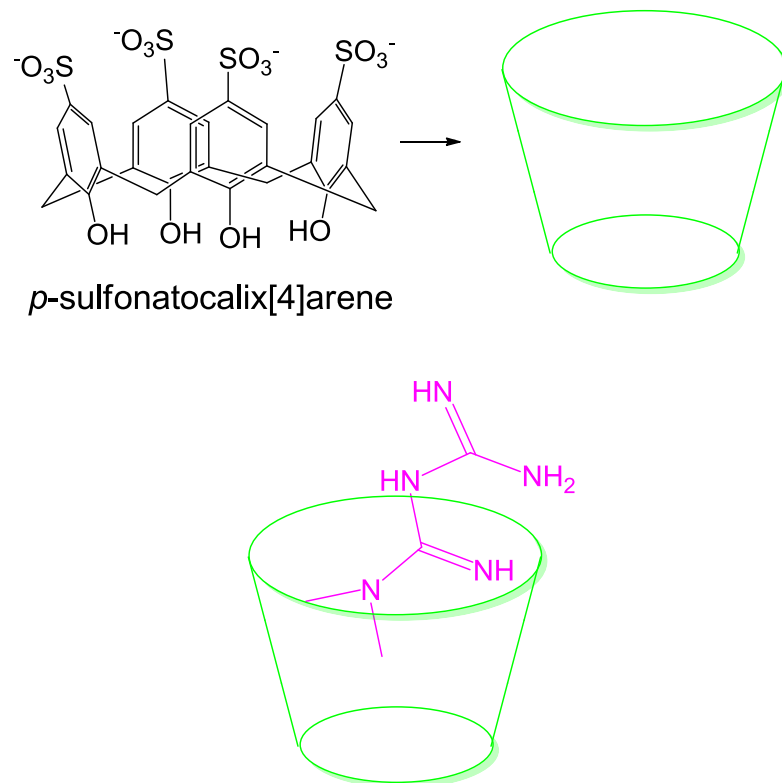


Figure 8: The host-guest complexation of metformin and *p*-sulfonatocalix[4]arene.

CHAPTER III
MATERIALS AND METHODS

Materials and Methods:

All chemicals were purchased from commercial sources and used as received. Solvents were purified by using a standard protocol, p-tert-butylcalix[4]arene, n-propanol, Chloroform, n-Hexane, Ethyl acetate, Petroleum ether, Dichloromethane was obtained from Loba Chem, Methanol from Fisher Chemicals, Tetrahydrofuran from Spectrochem.

Instruments used:

All chemicals and reagents were weighted on a weighing balance (Metler Toledo, Swiss made, (1mg-120mg+0.1 mg). Characterization of substituted products ^1H NMR, was carried out on a Bruker Avance II 400 Nuclear Magnetic Resonance (FT-NMR) using CDCl_3 as solvent and TMS as internal standard. Resonances are reported in ppm downfield from TMS. IR Spectra was carried out on Fourier Transform-Infrared Spectrophotometer (FTIR) Bruker Model: Tensor 27, using KBr pellet method for the solid sample.

Synthesis of H-2:

To a 250 mL R.B.F, calix[4]arene (5 g), K_2CO_3 (10.64 g), PrI (3.68 mL) were added and mixed. When they all get soluble, acetone (150 mL) was added and kept for reflux for 24 hours at 70°C temperature. Upon monitoring TLC, the reaction mixture acetone was filtered, the filtrate was collected in filtration flask. Collected filtrate was transferred to a 50 mL beaker and it was kept on oil bath at 70°C to evaporate acetone, which lead to a residue containing some amount of inorganic compound [K_2CO_3], to remove it chloroform and H_2O was added to the residue and mixed vigorously in the separating funnel. Two immiscible solvent phases (CHCl_3 and H_2O) separates out the organic and inorganic compounds. Organic layer was extracted with CHCl_3 in a 50 mL beaker and the other layer containing K_2CO_3 in water was discarded. The organic layer contains product was filtered through anhydrous sodium sulphate to remove the remaining water in organic layer. It was again concentrated by keeping it on oil bath at 70°C to evaporate chloroform followed by recrystallization carried out by adding 3 to 5 mL of methanol.

Characterstics of H-2: Colourless crystalline compound; yield=3.58 g; ^1H NMR (CDCl_3 400 MHz) δ (ppm): 1.00 (s, 18H, $\text{C}(\text{CH}_3)_3$), 1.25 (t, $J=6.08$ Hz, 6H, CH_3), 1.26 (s, 18H, $\text{C}(\text{CH}_3)_3$), 2.01 (m, 4H, CH_2), 3.43 (d, $J=13.4$ Hz, 4H, ArCH_2Ar), 3.95 (t,

J=6.12 Hz, 4H, OCH₂), 4.20 (d, J=13.4 Hz, 4H, ArCH₂Ar), 6.83 (s, 4H, ArH), 7.02 (s, 4H, ArH); FTIR (ν_{\max} KBr, cm⁻¹), 1596 cm⁻¹ C-O str; FAB-MS m/z 810 (M⁺).

Synthesis of H-3:

To a 100 mL RBF, NaH (2.65 g) (60% NaH dispersed in mineral oil) and hexane was added and kept for few minutes to wash away the grease. After that hexane was removed with the help of dropper. Now calix[4]arene (4 g), PrI (2.9 mL) was added in 20-25 mL of DMF solvent and kept for stirring under anhydrous condition for 32 hours. After monitoring TLC, upon completion the reaction mixture was poured into ice cold. The residue was filtered and dried. The product was not totally soluble in chloroform since some impurities were present, to remove those impurities chloroform was added and transferred to a separating funnel (250 mL) with water. It was vigorously shaken to separate organic and inorganic layer. Product was recovered by extracting it with organic layer in a (3×50) mL CHCl₃. Chloroform layer containing product was again filtered through anhydrous sodium sulphate to remove excess of water in product and it was collected in a 100 mL beaker. The beaker was kept on oil bath to distilled chloroform followed by recrystallization in methanol.

Characteristics of H-3: White crystalline compound; yield=3.06 g; ¹H NMR (CDCl₃ 400 MHz) δ (ppm):), 0.9 (t, J=7.32 Hz, 12H, CH₃), 1.06 (s, 36H, C(CH₃)), 2.01 (m, 8H, CH₂), 3.05 (d, J=12.8 Hz, 4H, ArCH₂Ar), 3.80 (t, J=4.28 Hz, 8H, OCH₂), 4.35 (d, J=12.2 Hz, 4H, ArCH₂Ar), 6.83 (s, 8H, ArH); FAB-MS m/z 810 (M⁺).

Synthesis of H-4:

To a 500 mL R.B.F, calix[4]arene (10 g), K₂CO₃(6.53 g) were added in acetone (50 mL). After that NaI (8 g) was added and kept for reflux with stirring on at 70°C. The reaction mixture was refluxed for 4 h. After completion of the reaction (TLC), the reaction mixture was filtered through celite bed on the surface of the filter paper under reaction. The solvent was then removed under reduce pressure and recrystallized from methanol to furnish to the residue 5,11,17,23-tert-butyl-syn-25,27-bis(cyanomethoxy)-26,28-dihydroxycalix[4]arene.

Characteristics of H-4: Yield=7.87 g; colourless solid; ^1H NMR (CDCl_3 , 400MHz) δ (ppm): 0.86(18H, s, $\text{C}(\text{CH}_3)_3$), 1.31 (18H, s, $\text{C}(\text{CH}_3)_3$), 3.43 (4H, d, $J=13.4$ Hz, ArCH_2Ar), 4.20 (4H, d, $J=13.4$ Hz, ArCH_2Ar), 5.00 (4H, s, OCH_2CN), 5.54 (2H, s, ArOH), 6.40 (4H, s, ArH) and 7.15 (4H, s, ArH); FTIR ($\nu_{\text{max}}\text{KBr}, \text{cm}^{-1}$), 2269 ($\text{C}\equiv\text{N}$), FAB-MS m/z 726 (M^+).

Synthesis of H-5:

To a 100 mL R.B.F, NaH (60% NaH dispersed in mineral oil) (450 mg) and hexane were added and kept for 10 minutes to wash away the grease and to make the NaH pure free of mineral oil layer where hexane was removed by dropper. After that **H-5** (2.178 g) and DMF (20-25 mL) were added and kept for stirring under anhydrous condition for 7 days. After the completion of reaction monitored by TLC, the reaction workup was done. To the reaction mixture, water was added and filtered in Buchner funnel, residue was collected in 50 mL beaker and it was dissolved in chloroform.

Since, some impurities have been seen on dissolving it in chloroform, the reaction mixture was again dissolved in water and the whole mixture was transferred to a separating funnel (250 mL) where two phases separated out. Organic layer was extracted and passed through anhydrous sodium sulphate to remove traces of water. Filtrate was collected in a conical flask(100 mL), it was distilled followed by recrystallization in 2-3 mL of methanol to furnish 5,11,17,23,- tetra-tert-butyl-25,27-dicyanomethoxy-26,28-dipropoxycalix[4]arene.

Characteristics of H-5: Yield=0.31 g, white solid; mp; ^1H NMR(CDCl_3 , 400MHz) δ (ppm): 0.80 (s, 18H, $\text{C}(\text{CH}_3)_3$), 1.03 (t, $J=7.36$ Hz, 6H, CH_3) 1.35 (s, 18H, $\text{C}(\text{CH}_3)_3$), 1.9 (m, 4H, CH_2), 3.23 (d, $J=13.4$ Hz, 4H, ArCH_2Ar), 3.73 (t, 4H, OCH_2), 4.38 (d, $J=13.4$ Hz, 4H, ArCH_2Ar), 5.00 (s, 4H, OCH_2CN), 6.40 (s, 4H, ArH), 7.15 (s, 4H, ArH); FTIR ($\nu_{\text{max}}\text{KBr}, \text{cm}^{-1}$): 2269 ($\text{C}\equiv\text{N}$); FAB-MS m/z 810 (M^+).

Synthesis of H-6: To a 100 mL RBF, **H-4** (2.17 g), Cs_2CO_3 (2.93 g) and DMF (20-25 mL) were added and stirred, after few seconds stirring PrI (0.87 mL) was added and kept for stirring under anhydrous condition for seven days. TLC was monitored for completion of reaction. Upon completion of reaction, to the reaction

mixture water was added. After monitoring TLC, to the reaction mixture, water was added and filtered in Buchner funnel. Chloroform was added to the residue collected in 100 mL beaker and it was filtered through anhydrous sodium sulphate on filter paper to remove water. The reaction mixture was partially crystallized in chloroform followed by recrystallization in 2-3 mL of methanol to furnish **H-6** in 1,3-alternate conformation.

Characteristics of H-6: Yield=1.3 g, white solid; $^1\text{H NMR}$ (CDCl_3 , 400MHz) δ (ppm): 0.06 (t, $J=7.36$, 6H, CH_3), 1.12 (m, 4H, CH_2), 1.25 (s, 18H, $\text{C}(\text{CH}_3)_3$), 1.33(s, 18H, $\text{C}(\text{CH}_3)_3$), 3.2 (s,4H, OCH_2CN), 3.39 (t, $J=7.92$ Hz, 4H, OCH_2), 3.85 (d, $J=16.48$ Hz, 4H, ArCH_2Ar), 3.91 (d, $J=15.88$ Hz, 4H, ArCH_2Ar), 7.01 (s, 4H, ArH), 7.17 (s, 4H, ArH); FTIR (ν_{max} KBr, cm^{-1}): 2269 ($\text{C}\equiv\text{N}$); FAB-MS m/z 810 (M^+).

CHAPTER IV

RESULTS AND DISCUSSIONS

Result and Discussion:

4.1 Synthesis and Characterization of calix[4]arene derivative in cone and 1,3-alternate conformation:

Calix[4]arene was synthesized by condensation of p-tert-butylphenol with formaldehyde in presence of NaOH as base as per the reported method excess K_2CO_3 in acetone as solvent under reflux conditions (24 h) furnished 25,27-dipropoxy-26,28-dihydroxycalix[4]arene **H-2** upon recrystallization in CH_2Cl_2 : MeOH. (**Scheme 1**) The structure of the product was confirmed by FTIR, 1H NMR and Mass Spectrometry (MS). The FTIR showed absorption peak around at 3200-3600, 2900 and 1596 cm^{-1} characteristics of hydroxyl moiety and phenolic C-O str. 1H NMR spectra of **H-2** showed the presence of a triplet at δ 1.25 ppm (6H), multiplet at δ 2.01 ppm (4H) and a triplet at δ 3.95 ppm (4H) which are characteristics of CH_3 , CH_2 , and OCH_2 of propyl moiety, the presence of two singlet at δ 6.83 and 7.02 ppm for 4H is characteristic of meta-aromatic hydrogen. Further the presence of two singlets at δ 1.00 ppm and 1.26 ppm for 18H each characteristic of the methyl groups of t-Bu moiety of calix[4]arene, showing chemically non-equivalent t-Bu groups. A pair of doublet at δ 3.29 (J=16 Hz) and 4.29 (J=16 Hz) ppm, are separated by $1 > 0.7$ ppm, is characteristic of bridging methylene axial and equatorial protons in the syn-orientation of the phenolic groups in calix[4]arene. The EI-MS of **H-2** was characterized by a molecular ion peak at 732 (M^+). Thus, the spectroscopic data corroborate with the structure of **H-2**.

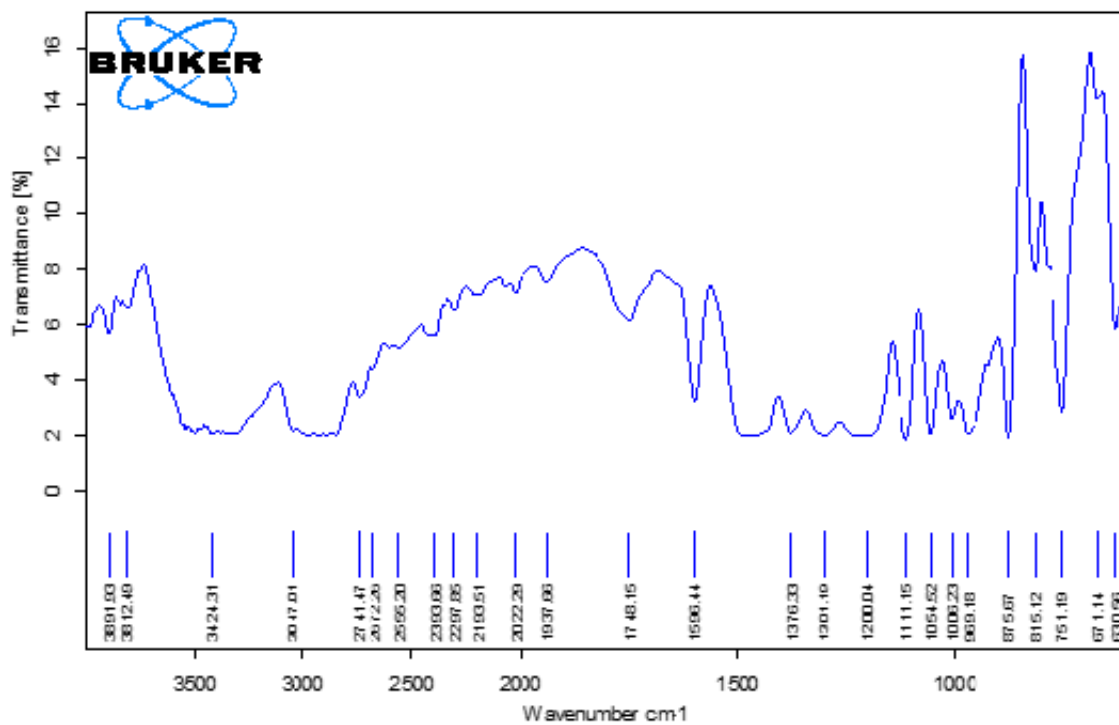


Figure 9: FTIR of calix[4]arene derivative H-2.

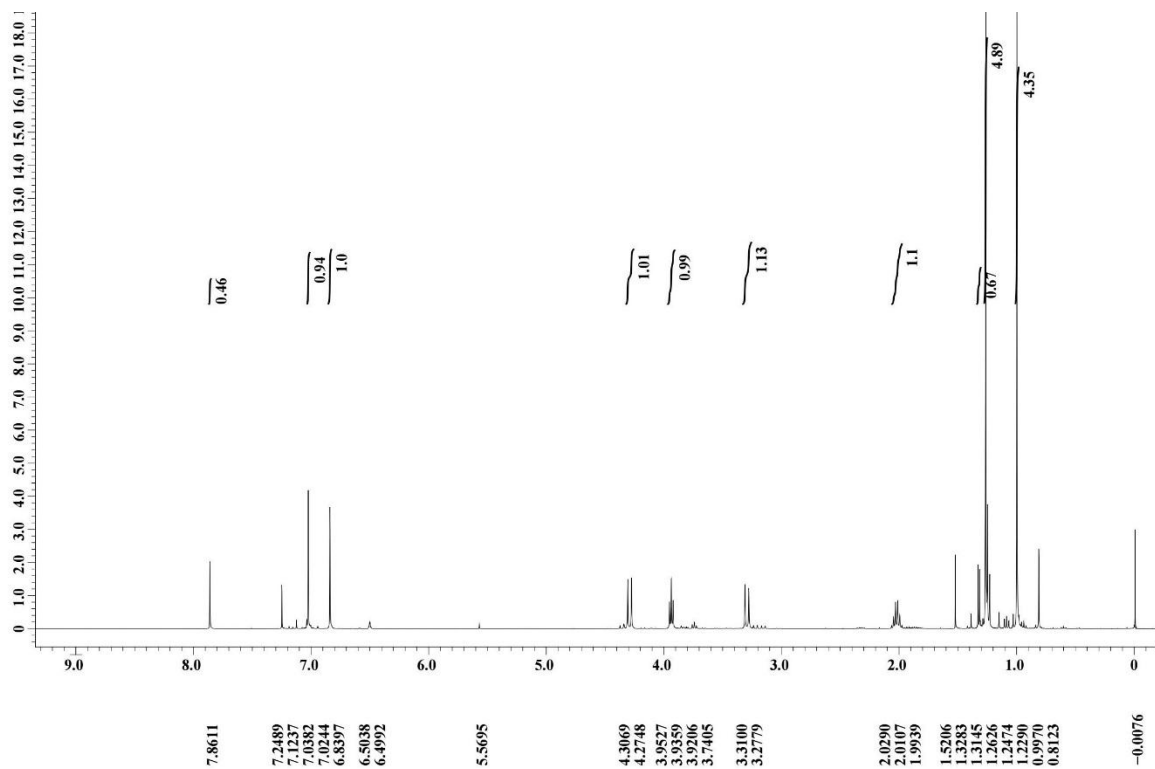


Figure 10: ¹H NMR spectra of H-2.

Using NaH as the base, alkylation of calix[4]arene (H-1) with propyl iodide in DMF as solvent at room temperature (48 h) under stirring furnished 25,26,27,28-

tetrapropoxycalix[4]arene **H-3** upon recrystallization in $\text{CH}_2\text{Cl}_2:\text{MeOH}$. The structure of the product was confirmed by FTIR, ^1H NMR and Mass Spectrometry (MS). The FTIR showed no absorption peak around at $3200\text{-}3600\text{ cm}^{-1}$. ^1H NMR spectra of **H-3** showed the presence of a triplet at δ 0.9 ppm (12H), multiplet at δ 2.01 ppm (8H) and a triplet at δ 3.80 ppm (8H) which are characteristics of CH_3 , CH_2 , and OCH_2 of propyl moiety. Further the presence of a singlet at δ 1.06 ppm for (36H) is characteristic of the t-Bu moiety of calix[4]arene symmetrical tetrasubstituted at phenolic moieties. A pair of doublet at δ 3.05 ($J=12.84\text{ Hz}$) and 4.35 ($J=12.2\text{ Hz}$) ppm, are separated by $>0.7\text{ ppm}$ is characteristic of bridging methylene axial and equatorial protons in the syn-orientation of the phenolic groups in **H-3**. The EI-MS of **H-3** was characterized by a molecular ion peak at 816 (M^+). Thus, the spectroscopic data corroborate with the structure of **H-3**.

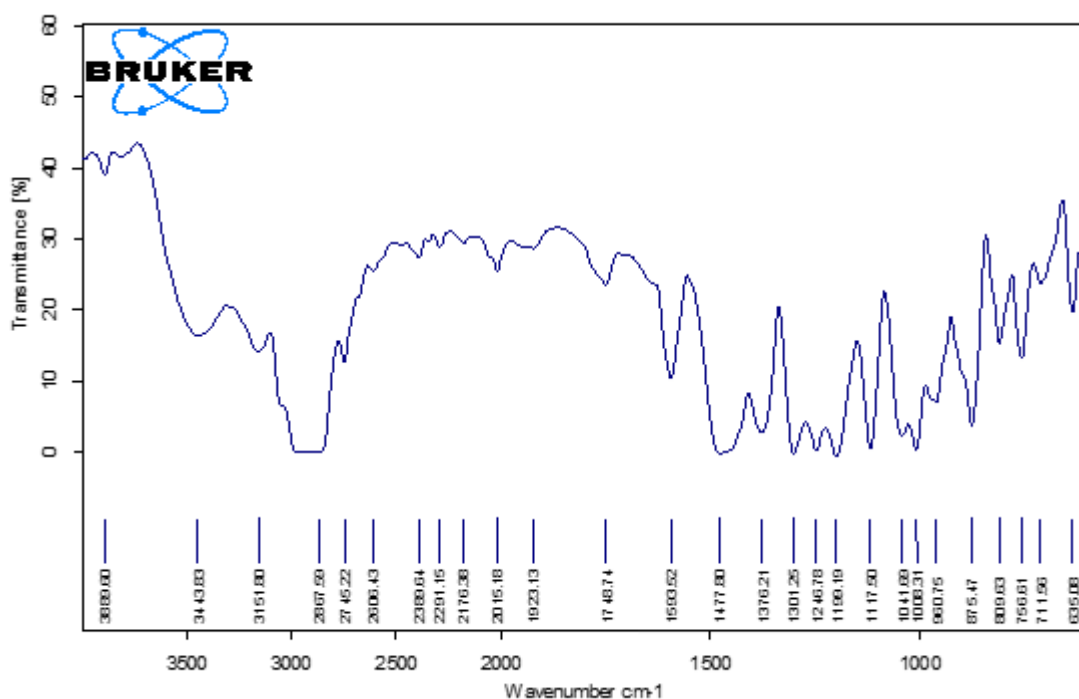


Figure 11: FTIR of calix[4]arene derivative **H-3**.

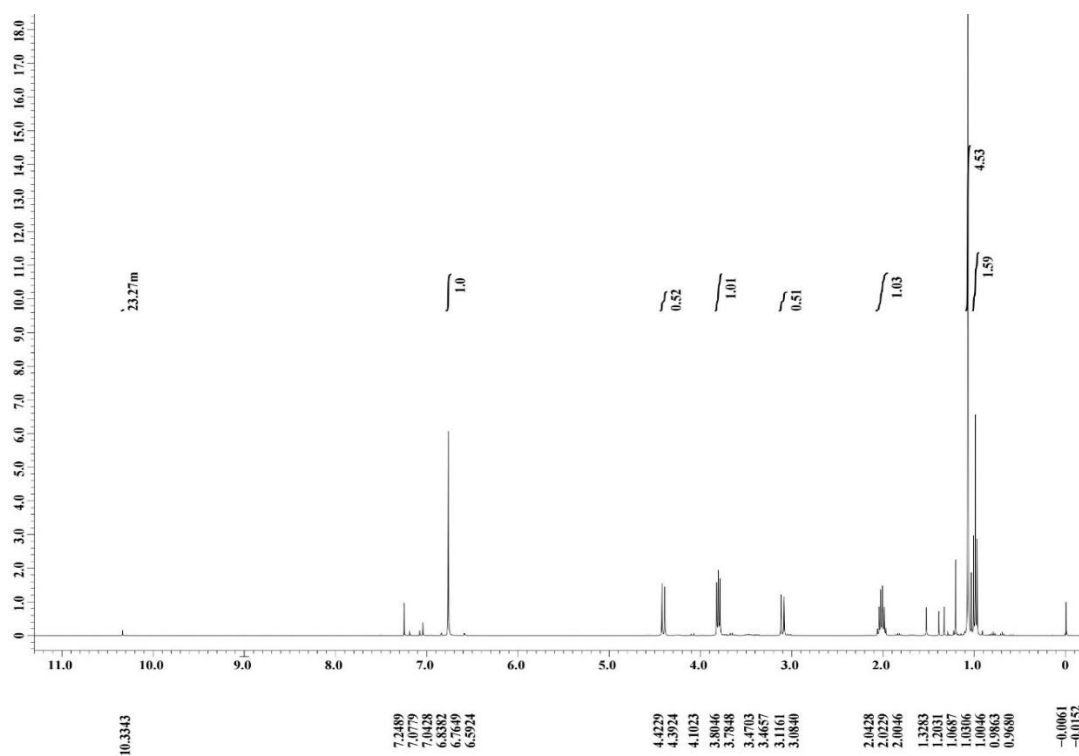


Figure 12: ^1H NMR spectra of **H-3**.

Alkylation of calix[4]arene with chloroacetonitrile/ $\text{NaI}/\text{K}_2\text{CO}_3$ (Collins and Vernon 1991) furnished compound **H-4** in cone conformation. Compound **H-4** was characterized by ^1H , FTIR and melting point characteristics. The FTIR showed absorption band at 2269 of ($\text{C}\equiv\text{N}$). ^1H NMR spectra of **H-4** showed the presence of a singlet at δ 4.79 ppm (4H), and δ 5.54 ppm (2H) which are characteristics of nitrile methylene and phenolic moieties in **H-4**, respectively. The presence of a singlet at δ 1.31 and 0.86 ppm for 18H are characteristics of t-Bu. Another singlet at δ 5.54 ppm for aromatic OH. Further the presence of two singlet at δ 6.71 and 7.10 ppm for **4H** is characteristic of meta-aromatic hydrogen. A pair of doublet at δ 3.43 ($J=13.4$ Hz) and 4.20 ($J=13.4$ Hz) ppm, separated by >0.7 ppm is characteristic of bridging methylene axial and equatorial protons in the syn-orientation of the phenolic groups in **H-4**. The EI-MS of **H-4** was characterized by a molecular ion peak at 726 (M^+). Thus, the spectroscopic data corroborate with the structure of **H-4**.

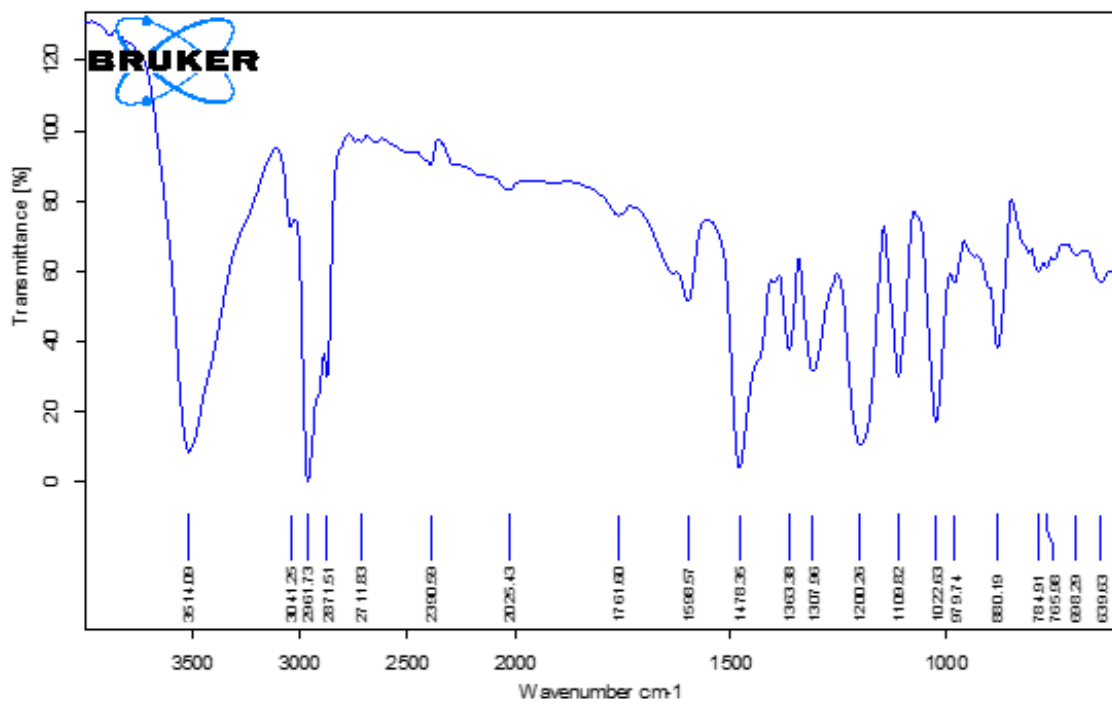


Figure 13: FTIR spectra of calix[4]arene derivative H-4.

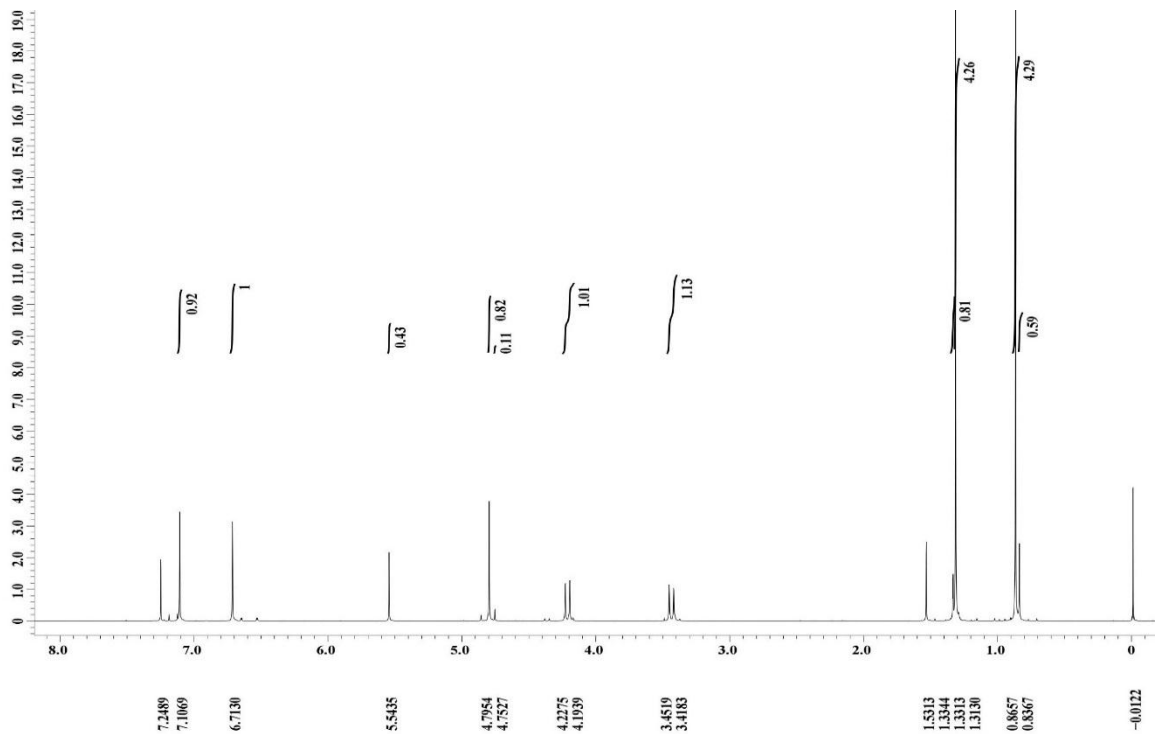


Figure 14: ¹H NMR spectra of H-4.

Using NaH as the base, alkylation of **H-4** with propyl iodide in DMF as solvent stirring at room temperature (7 days) furnished **H-5** upon recrystallization in CH₂Cl₂:MeOH. The structure of the product was confirmed by FTIR, ¹H NMR. The FTIR showed peak at 2269 of (C≡N). ¹H NMR spectra of **H-5** showed the presence of a singlet at δ 5.00 ppm for 2H corresponds to methoxyacetonitrile. The presence of a triplet at δ 1.03 ppm (6H), multiplet at δ 1.99 ppm (4H) and a triplet at δ 3.73 ppm (4H) which are characteristics of CH₃, CH₂, and CH₂ of propyl moiety. Two singlets at δ 6.40 and 7.15 ppm corresponds to 4H each, is characteristics of meta-aromatic hydrogen. Two singlet at δ 1.35 and 0.80 ppm for 18H is characteristic of t-Bu. Another singlet at δ 1.53 ppm for H₂O hydrogen. A pair of doublet at δ 3.23 (J=13.4) and 4.38 (J=13.4) ppm, separated by > 0.7 ppm is characteristic of bridging methylene axial and equatorial protons in the syn-orientation of the phenolic groups in **H-5**. The EI-MS of **H-5** was characterized by a molecular ion peak at 810 (M⁺). Thus, the spectroscopic data corroborate with the structure of **H-5**.

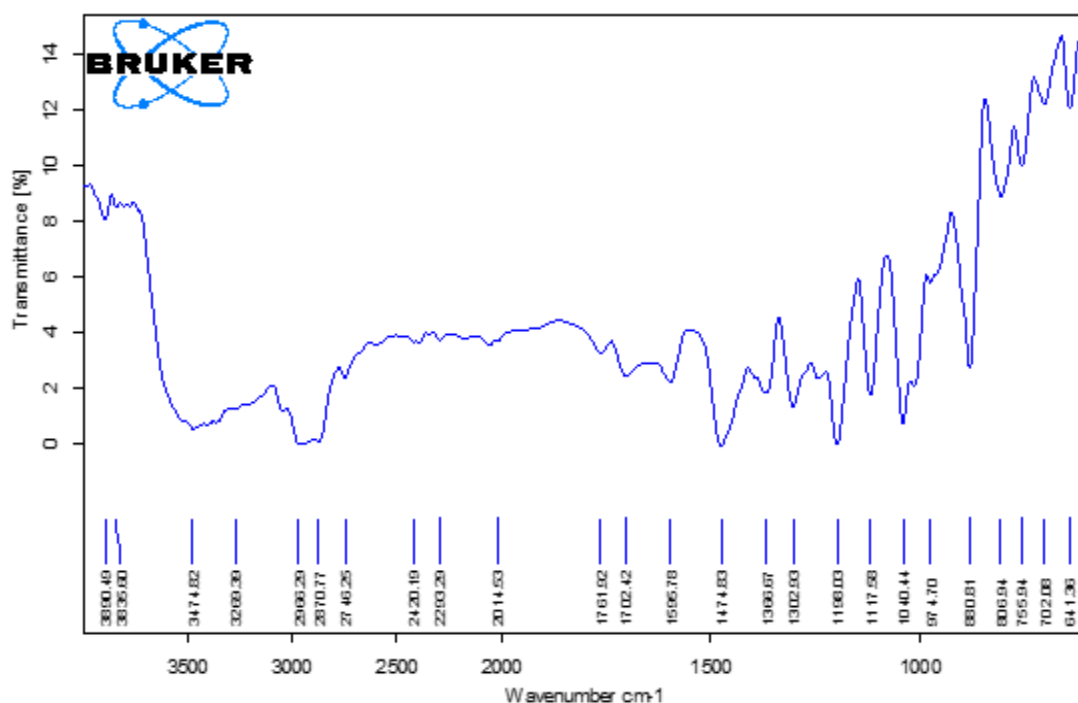


Figure 15: FTIR spectra of calix[4]arene derivative **H-5**.

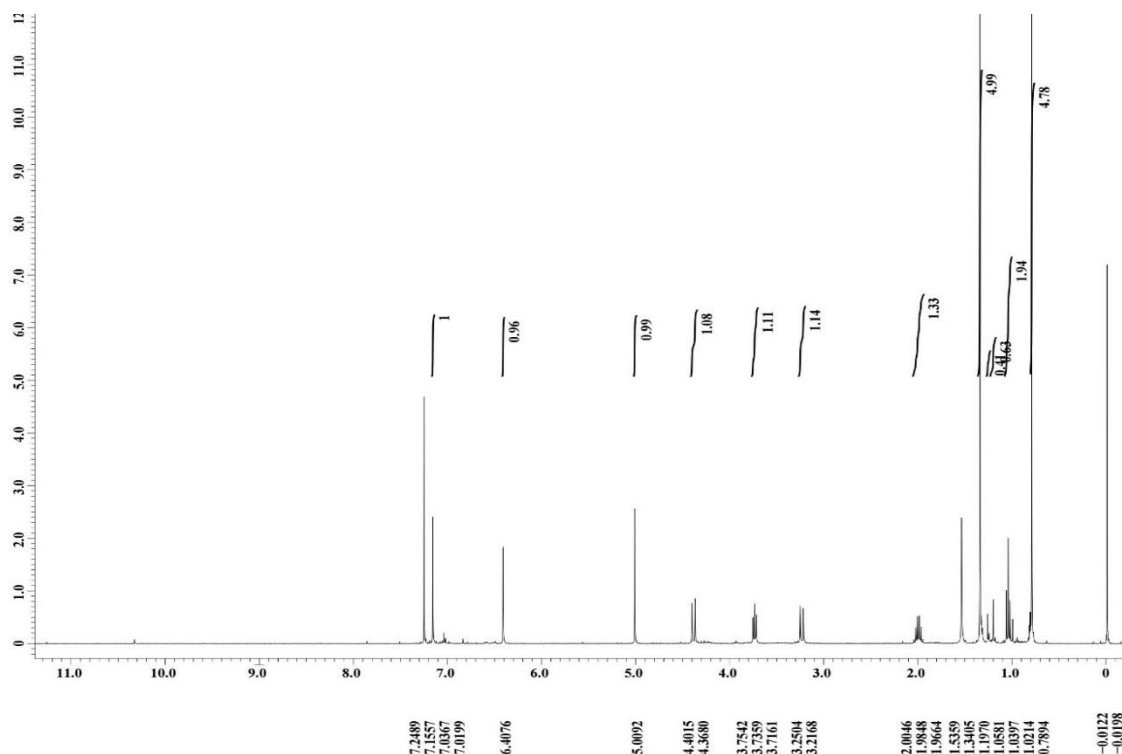


Figure 16: ^1H NMR spectra of **H-5**.

For further investigation of the conformational isomers on sensing of aromatic analytes, the bis(cyanomethoxy) derivative of calix[4]arene have been synthesized in 1,3-alternate (Babu,2009). Thus, alkylation of dicyanomethoxy derivatives **H-4** with propyl iodide in dry N,N-dimethylformamide (DMF) using cesium carbonate(Cs_2CO_3) as base, for 7 days resulted in the formation of compound **H-6**.The structure of the product was confirmed by FTIR, ^1H NMR and Mass Spectrometry (MS). The FTIR showed absorption band at 2269 of ($\text{C}\equiv\text{N}$). ^1H NMR spectra of **H-2** showed the presence of a triplet at δ 0.66 ppm (6H), multiplet at δ 1.12 ppm (4H) and a triplet at δ 3.39 ppm (4H) which are characteristics of CH_3 , CH_2 , and OCH_2 of propyl moiety. The presence of two singlet at δ 1.25 and 1.33 ppm for 18 H each characteristics of t-Bu moiety of calixarene, showing chemically non-equivalent t-Bu groups another singlet at δ 3.2ppm for 4H is characteristics of methoxyacetonitrile. Two doublets at δ 3.85 ($J=16.48\text{Hz}$) and 3.91 ($J=15.88\text{Hz}$) ppm separated by $< 0.6\text{ppm}$ is characteristic of bridging methylene axial and equatorial protons in the anti-orientation of the phenolic groups in **H-6**. Two singlet at δ 7.01 and 7.17 ppm corresponds to 4H is characteristic of meta-aromatic hydrogen. The EI-MS of **H-6** was characterized by a molecular ion peak at 810 (M^+).

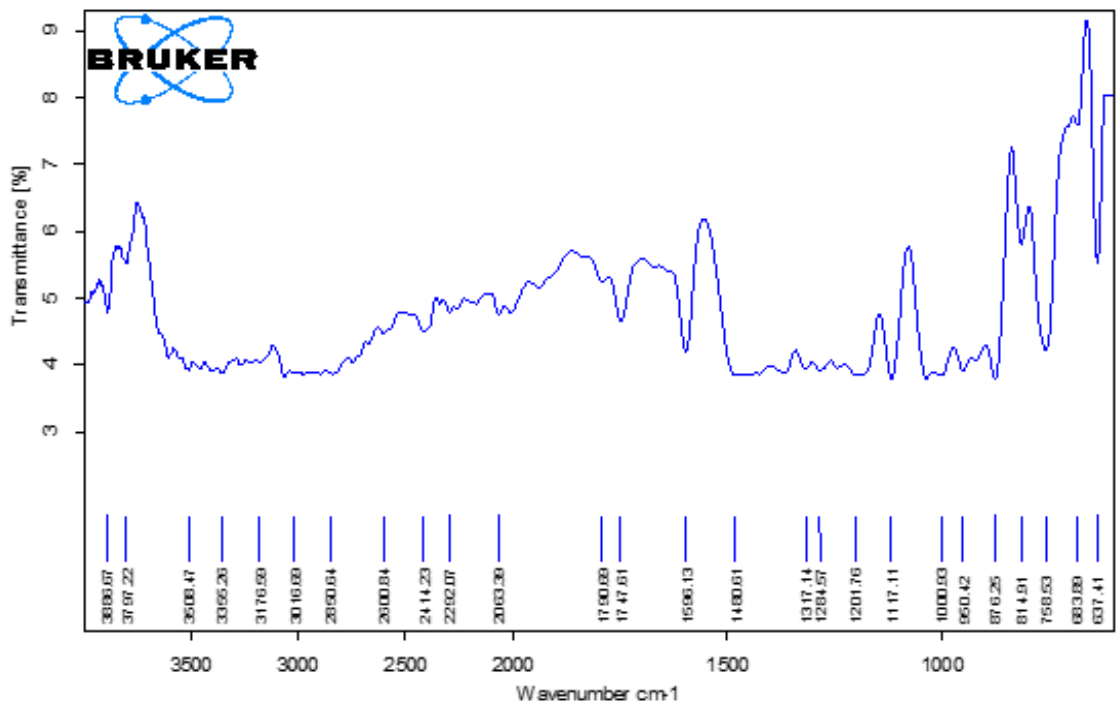


Figure 17: FTIR spectra of calix[4]arene derivative H-6.

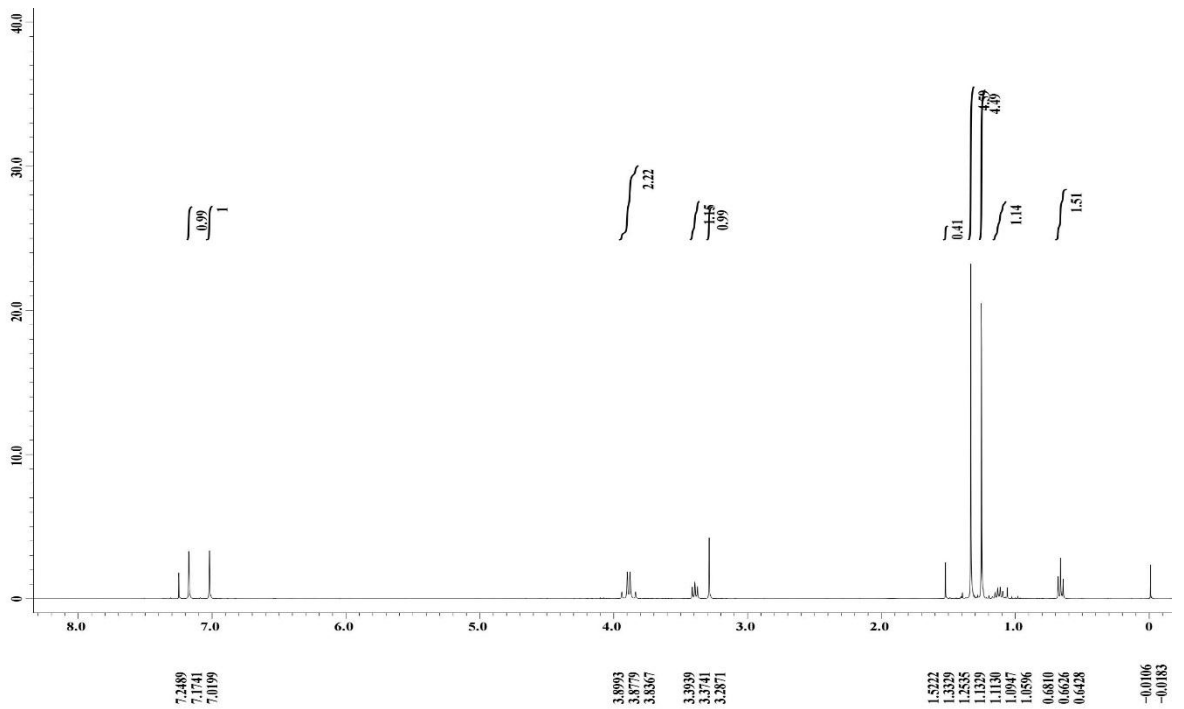
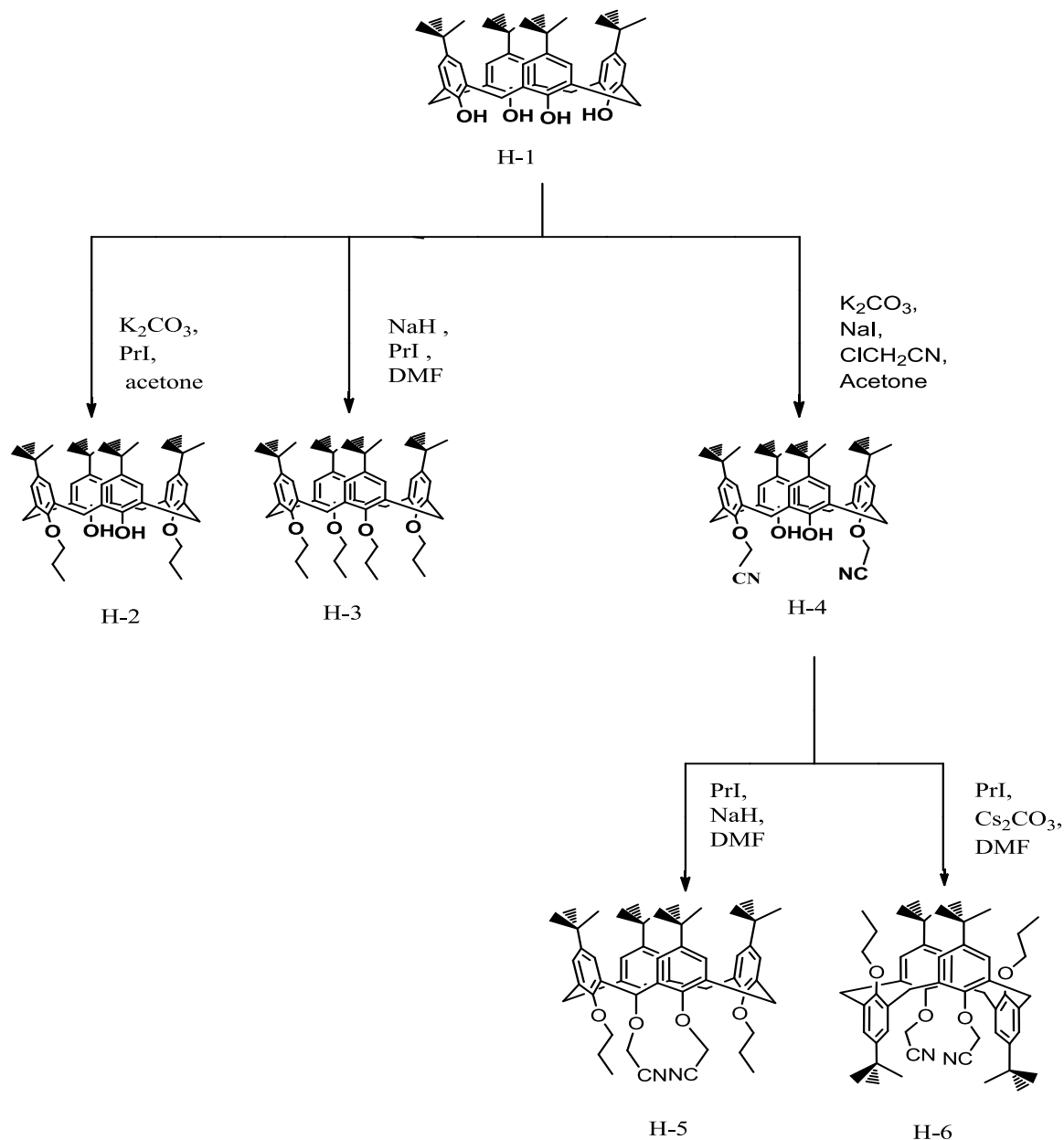


Figure 18: ¹H NMR spectra of H-6.



Scheme 4.1: Synthesis of calix[4]arene derivative in cone and 1,3-alternate conformation.

UV-Visible Studies and stability constant:

UV-Visible studies of **H-2** were studied in presence of metformin (0-10 equiv.) in CH₂Cl₂:MeOH (1:9, v/v). The UV-Visible spectra of **H-2** showed an absorption band at 281 and 281.5 nm. For the evaluation purpose absorption band at λ_{\max} =281 nm were used for the analysis. Upon addition of metformin (0-10 equiv.), the absorption band at λ_{\max} =281 nm showed a hyperchromic shift and (**Figure 19**). This is attributed to the formation of the host-guest complex between **H-2** and

metformin. Further the stability constant were calculated using Benesi-Hildebrand equation. The plot of the linearized form of Benesi-Hildebrand equation is shown in (Figure 20). The stability constant for **H-2** and metformin 1:1 complex is 2.19×10^4 M^{-1} .

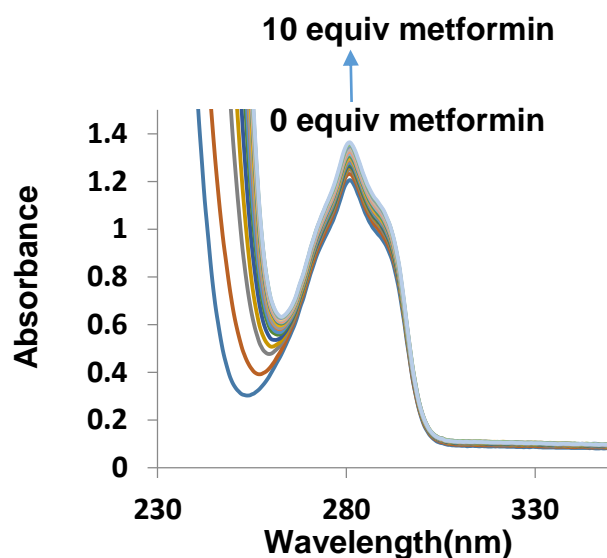


Figure 19: UV-Visible absorption changes upon addition of 0 to 10 equivalent metformin to **H-2** (1×10^{-4}) in methanol:chloroform 9:1 (v/v).

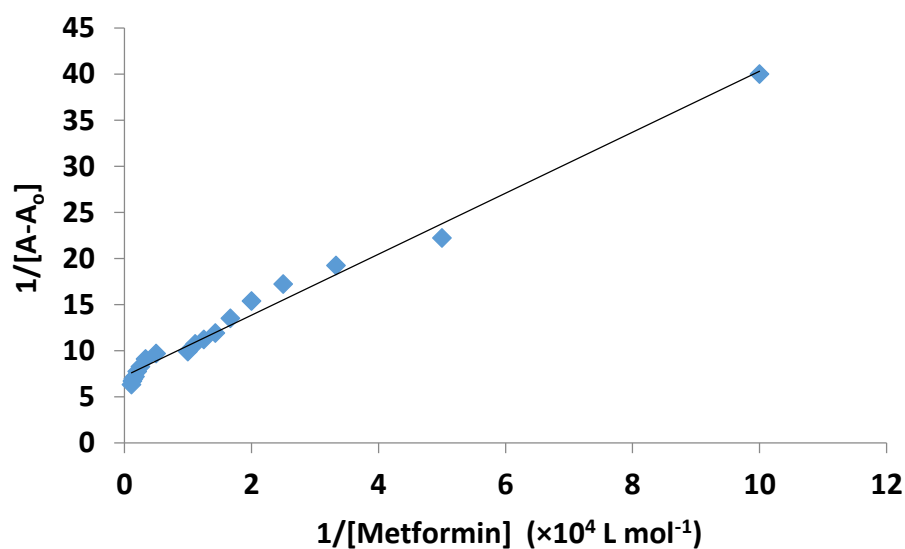


Figure 20: Association constant curve of **H-2** for metformin determined by UV-Visible method.

UV-Visible studies of **H-3** in presence of metformin (0-10 equiv.) in CH₂Cl₂: MeOH (1:9, v/v) was carried out for host-guest binding. The UV-Visible spectra of **H-3** showed an absorption band at 281 nm. For the evaluation purpose absorption band at $\lambda_{\text{max}}=281$ nm were used for the analysis. Upon addition of metformin (0-10 equiv.), the absorption band at $\lambda_{\text{max}}=281$ nm showed a hyperchromic shift (**Figure 21**). This is attributed to the formation of the host-guest complex between **H-3** and metformin. Further the stability constant were calculated using Benesi-Hildebrand equation. The plot of the linearized form of Benesi-Hildebrand equation is shown in (**Figure 22**). The stability constant for **H-3** and metformin 1:1 complex is 1.01×10^5 M⁻¹.

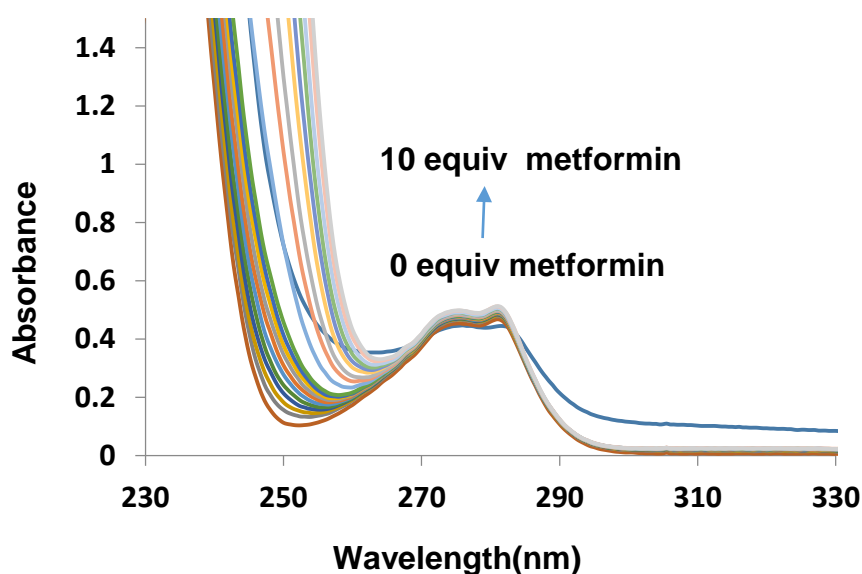


Figure 21: UV-Visible absorption changes upon addition of 0 to 10 equivalent metformin to **H-3** (1×10^{-4}) in methanol:chloroform 9:1 (v/v).

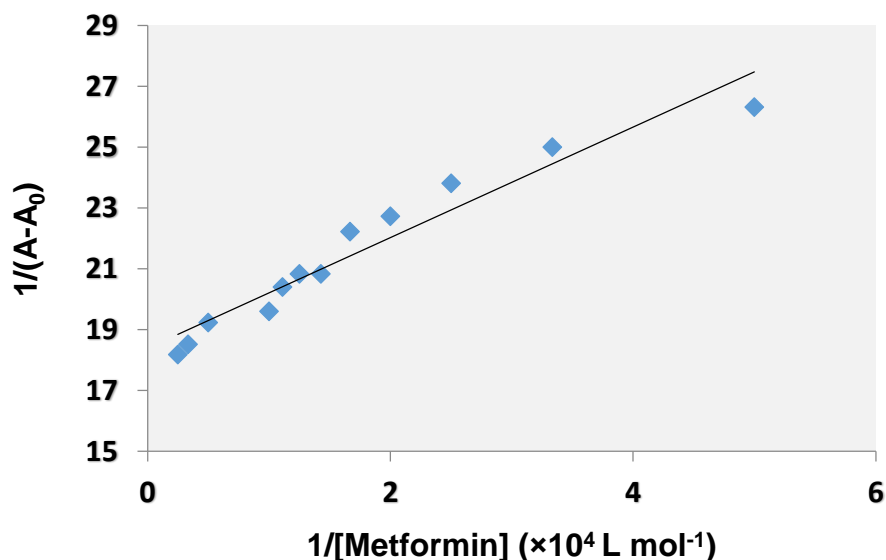


Figure 22: Association constant curve of **H-3** for metformin determined by UV-Vis method.

UV-Visible studies of **H-4** were studied in presence of metformin (0-10 equiv.) in CH₂Cl₂:MeOH (1:9, v/v). The UV-Visible spectra of **H-4** showed an absorption band at 281 and 280.5 nm. For the evaluation purpose absorption band at $\lambda_{\max}=280.5$ nm were used for the analysis. Upon addition of metformin (0-10 equiv.), the absorption band at $\lambda_{\max}=281$ nm showed a hyperchromic shift (**Figure 23**). This is attributed to the formation of the host-guest complex between **H-4** and metformin. Further the stability constant were calculated using Benesi-Hildebrand equation. The plot of the linearized form of Benesi-Hildebrand equation is shown in (**Figure 24**). The stability constant for **H-4** and metformin 1:1 complex is 3.53×10^4 M⁻¹.

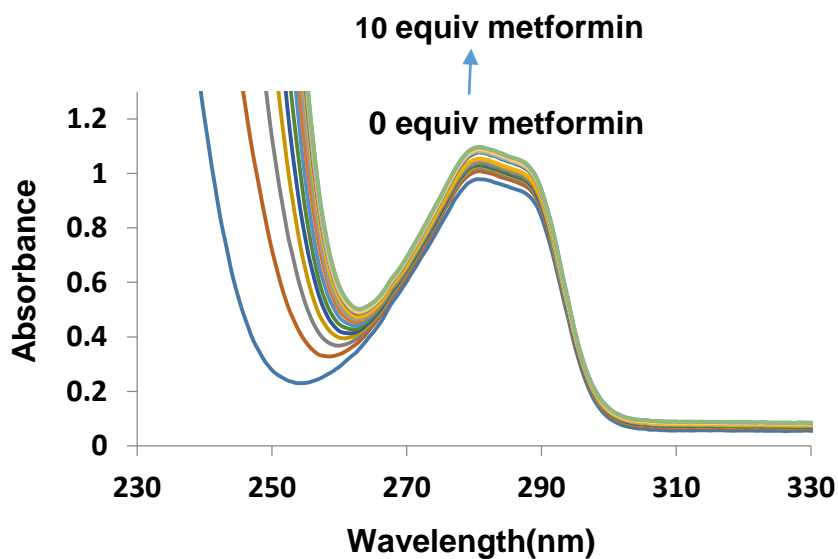


Figure 23: UV-Visible absorption changes upon addition of 0 to 10 equivalent metformin to **H-4** (1×10^{-4}) in methanol: chloroform 9:1 (v/v).

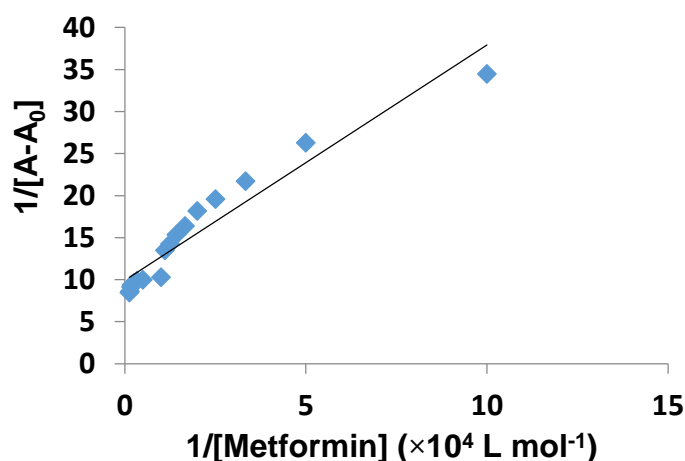


Figure 24: Association constant curve of **H-4** for metformin determined by UV-Vis method.

UV-Visible studies of **H-6** were studied in presence of metformin (0-10 equiv.) in $\text{CH}_2\text{Cl}_2:\text{MeOH}$ (1:9, v/v). The UV-Visible spectra of **H-6** showed an absorption band at 269.5 and 270 nm. For the evaluation purpose absorption band at $\lambda_{\text{max}}=269.5$ nm were used for the analysis. Upon addition of metformin (0-10 equiv.), the absorption band at $\lambda_{\text{max}}=281$ nm showed a hyperchromic shift (**Figure 25**). This is attributed to the formation of the host-guest complex between **H-6** and

metformin. Further the stability constant were calculated using Benesi-Hildebrand equation. The plot of the linearized form of Benesi-Hildebrand equation is shown in (Figure 26). The stability constant for **H-6** and metformin 1:1 complex is $5.15 \times 10^4 \text{ M}^{-1}$.

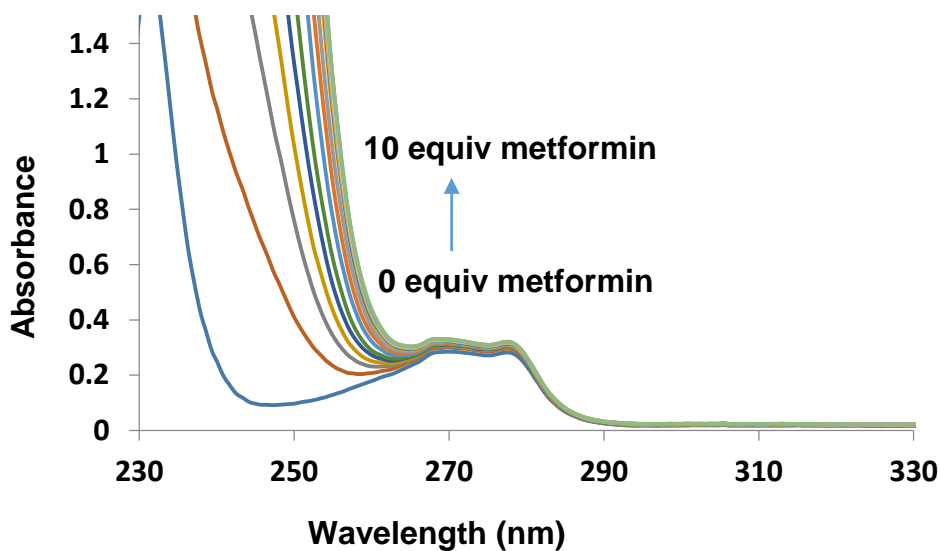


Figure 25: UV-Visible absorption changes upon addition of 0 to 10 equivalent metformin to **H-6** (1×10^{-4}) in methanol:chloroform 9:1 (v/v).

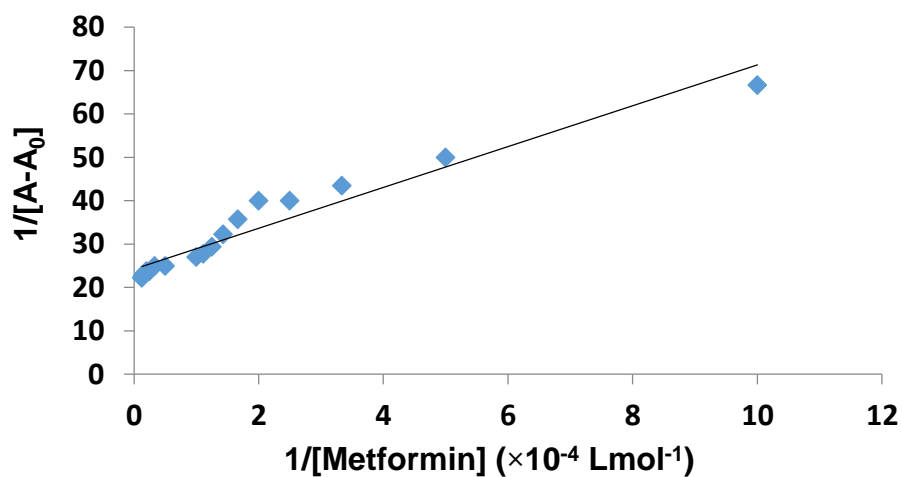


Figure 26: Association constant curve of **H-6** for metformin determined by UV-Vis method.

Association constant calculated for different calix[4]arene derivatives using Benesi-Hildebrand equation i.e.

$$\frac{1}{(A - A_0)} = \frac{1}{K (A_{\max} - A_0)[G]} + \frac{1}{(A_{\max} - A_0)}$$

The result of the stability constant K, for the association behaviour of metformin with **H 2-6**, is tabulated in **table 1**. The result show that **H-3** and **H-4** forms a stronger inclusion complex with metformin which indicates that cone conformation of dipropylcalix[4]arene and dinitrilecalix[4]arene with the common phenol moiety has a role to play in metformin inclusion. **H-6** which indicates dinitrilecalix[4]arene of 1,3,alternate conformation bind metformin strongly.

Table 4.1: Stability constant for Host-Guset complexation of calix[4]arene derivative **H-2-6** with metformin.

HOST	GUEST (Metformin)
H-2	2.19x 10 ⁴
H-3	1.01 x10 ⁵
H-4	3.53 x10 ⁴
H-6	5.15 x10 ⁴

CHAPTER V

CONCLUSIONS

Conclusion

The study on metformin inclusion using UV-Visible study showed a significant effect of phenolic hydroxyl moiety, conformation of calix[4]arene and lower rim derivatives. Further studies are required to analyze the association behaviour of **H 2-6** with metformin by ^1H NMR titration and Isothermal Calorimetry (ITC) studies.

REFERENCES

REFERENCES:

- Chang-Chen, K., Mullur, R., and Bernal-Mizrachi, E. (2008). β -Cell Failure as a Complication of Diabetes. *Reviews in Endocrine and Metabolic Disorders*, 9, 329.
- Collins, W., and Vernon, R. (1991). Orogeny Associated with Anticlockwise Ptt Paths: Evidence from Low-P, High-T Metamorphic Terranes in the Arunta Inlier, Central Australia. *Geology*, 19, 835-838.
- Duan, Q., Cao, Y., Li, Y., Hu, X., Xiao, T. (2013). Ph-Responsive Supramolecular Vesicles Based on Water-Soluble Pillar [6] Arene and Ferrocene Derivative for Drug Delivery. *Journal of the American Chemical Society*, 135, 10542-10549.
- Guo, D.-S., Zhang, H.-Q., Ding, F., and Liu, Y. (2012). Thermodynamic Origins of Selective Binding Affinity between P-Sulfonatocalix [4, 5] Arenes with Biguanidiniums. *Organic & biomolecular chemistry*, 10, 1527-1536.
- Gutsche, and David, C. (2008). *Calixarenes: An Introduction*: Royal Society of Chemistry.
- Gutsche, David, C., Levine, and A, J. (1982). Calixarenes. 6. Synthesis of a Functionalizable Calix [4] Arene in a Conformationally Rigid Cone Conformation. *Journal of the American Chemical Society*, 104, 2652-2653.
- Kataky, R., Kelly, P. M., Parker, D., and Patti, A. F. (1994). Selective Binding and Sensing of Guanidinium Ions by Lipophilic Cyclodextrins. *Journal of the Chemical Society, Perkin Transactions 2*, 2381-2382.
- Lee, M., Lee, S.-J., and Jiang, L.-H. (2004). Stimuli-Responsive Supramolecular Nanocapsules from Amphiphilic Calixarene Assembly. *Journal of the American Chemical Society*, 126, 12724-12725.
- Liu, Y., Wang, H., Wang, L.-H., Li, Z., Zhang, H.-Y. (2003). Synthesis of Novel P-Tert-Butyl-Calix [4] Arene Derivatives and Their Cation Binding Ability: Chromogenic Effect Upon Side Arms Binding. *Tetrahedron*, 59, 7967-7972.
- MacGillivray, B. C., and Macartney, D. H. (2013). Cucurbit [7] Uril Host–Guest Complexes with Biguanidinium Cations in Aqueous Solution. *European Journal of Organic Chemistry*, 2013, 2573-2582.

- Roselet, S. L., and Premakumari, J. (2015). Studies on Metformin Hydrochloride and Alpha-Cyclodextrin Inclusion Complexes. *Green Chemistry & Technology Letters*, 1, 48-53.
- Scheen, A. J. (1996). Clinical Pharmacokinetics of Metformin. *Clinical pharmacokinetics*, 30, 359-371.
- Steed, J. W., and Atwood, J. L. (2013). *Supramolecular Chemistry*: John Wiley & Sons.
- Stewart, D. R., Krawiec, M., Kashyap, R. P., Watson, W. H., and Gutsche, C. D. (1995). Conformational Characteristics of Ethers and Esters of P-Tert-Butylcalix [5] Arene. *Journal of the American Chemical Society*, 117, 586-601.
- Tripathi, K. (2013). *Essentials of Medical Pharmacology*: JP Medical Ltd.
- Tu, C., Zhu, L., Li, P., Chen, Y., Su, Y. (2011). Supramolecular Polymeric Micelles by the Host–Guest Interaction of Star-Like Calix [4] Arene and Chlorin E6 for Photodynamic Therapy. *Chemical Communications*, 47, 6063-6065.
- Wang, C., Li, Z., Cao, D., Zhao, Y. L., Gaines, J. W. (2012). Stimulated Release of Size-Selected Cargos in Succession from Mesoporous Silica Nanoparticles. *Angewandte Chemie International Edition*, 51, 5460-5465.
- Wheate, N. J., Abbott, G. M., Tate, R. J., Clements, C. J., Edrada-Ebel, R. (2009). Side-on Binding of P-Sulphonatocalix [4] Arene to the Dinuclear Platinum Complex Trans- $[\{PtCl(NH_3)_2\}_2\mu-Dpzm]^{2+}$ and Its Implications for Anticancer Drug Delivery. *Journal of inorganic biochemistry*, 103, 448-454.
- Yang, Y.-W. (2011). Towards Biocompatible Nanovalves Based on Mesoporous Silica Nanoparticles. *MedChemComm*, 2, 1033-1049.
- Zhou, Y., Li, H., and Yang, Y.-W. (2015). Controlled Drug Delivery Systems Based on Calixarenes. *Chinese Chemical Letters*, 26, 825-828.